



# Four new Solenogastres (Mollusca, Aplacophora) from the South China Sea and paraphyly of Proneomeniidae Simroth, 1893

M. Carmen Cobo<sup>A,\*</sup>, Emily L. McLaughlin<sup>A</sup> and Kevin M. Kocot<sup>A,B</sup>

For full list of author affiliations and declarations see end of paper

#### \*Correspondence to:

M. Carmen Cobo Department of Biological Sciences, The University of Alabama, Tuscaloosa, AL. USA

**Handling Editor:** 

Email: mcobollovo@ua.edu

Nerida Wilson

Received: 22 November 2022 Accepted: 14 April 2023 Published: 29 May 2023

#### Cite this:

Cobo MC et al. (2023) Invertebrate Systematics 37(5), 301-333. doi:10.1071/IS22062

© 2023 The Author(s) (or their employer(s)). Published by CSIRO Publishing.

#### **ABSTRACT**

Solenogastres and Caudofoveata (Aplacophora) remain some of the least known molluscs, despite ubiquity in the marine environment and importance in understanding molluscan evolution. The use of new morphological techniques and development of DNA barcode libraries have helped make specimen identification easier. However, for solenogasters, using histology for identification and adequate description of species remains necessary in most cases. This, together with the facts that knowledge about solenogaster species distributions is biased and that most species were described from one or very few individuals, explains why many open questions about the actual distribution, intra- and interspecific variability, etc., remain. We performed an integrative taxonomic study of eight specimens of solenogasters from the South China Sea (West Pacific Ocean) thatresulted in the identification of four new species of Proneomeniidae. Species identification and description following the established diagnostic characters were straightforward. However, phylogenetic analysis of molecular data obtained from these specimens and other members of Proneomeniidae indicate that the family is polyphyletic. We recovered representatives of two other families, Epimeniidae (Epimenia) and Strophomeniidae (Anamenia), nested within Proneomeniidae with strong support. Ancestral character state reconstruction indicates that characters commonly used in solenogaster taxonomy, such as the radula and foregut glands, may be more evolutionarily labile in this group than previously known. Therefore our work fills knowledge gaps regarding the diversity and distribution of members of this family but raises important questions about solenogaster taxonomy and systematics that should be further assessed with additional markers and broader taxon sampling.

ZooBank: urn:lsid:zoobank.org:pub:BCADACD6-9AD0-442A-AD64-031BA8D88599

Keywords: barcoding, biodiversity, mitochondrial DNA, Mollusca, morphology, south-west Pacific, systematics, taxonomy.

## Introduction

Aplacophora (Solenogastres + Caudofoveata) is a fascinating group of animals due to the significance in understanding the evolutionary history of the phylum Mollusca (Kocot et al. 2011, 2019; Smith et al. 2011; Vinther et al. 2012; Salvini-Plawen and Steiner 2014; Mikkelsen et al. 2019), unusual morphology with respect to other molluscs and ubiquity in the marine environment (García-Álvarez and Salvini-Plawen 2007; Todt 2013; Mikkelsen et al. 2019). However, this remains as one of the least known groups of molluscs, with uncertainties about the variability and evolutionary significance of some important characters such as the radulae and glands associated with the digestive system. Likewise, the real distribution and diversity are poorly known with only 449 species described (307 solenogasters and 142 caudofoveates), whereas the real number is estimated to be ten times higher than this (Todt 2013; estimation based only on specimens stored in museum collections).

One of the reasons for this lack of knowledge relates to the methodological requirements for studying these organisms. Taxonomic investigation of these worm-shaped animals involves the use of time-consuming techniques to describe certain internal organs

(e.g. the radula, digestive glands and reproductive system) and the small, fragile spines and scales (sclerites) that cover the bodies. This is especially challenging for solenogasters where, due to the generally small size and diagnostic characters used in the taxonomy (García-Álvarez and Salvini-Plawen 2007), histology is usually necessary to identify specimens even to family level. Solenogastres lack regional differentiation and therefore the external aspect is determined mainly by size (0.5-300 mm in length) and the appearance given by the sclerites that may or may not protrude from the cuticle. Most solenogasters are yellow, white or brownish but some species may have brighter colourations (e.g. Scheltema and Jebb 1994; Salvini-Plawen 1997). In the same way, certain solenogasters have cuticular keels, bumps or a posterior digitiform projection. Such distinctive traits occur in distantly related groups and although important for species identification, these are generally not diagnostic of higher taxa. Therefore, for a first classification into morphospecies, the general external appearance is important, and several authors have highlighted the usefulness of this and the sclerites to discern between lineages (Scheltema et al. 2012; Kocot and Todt 2014; Bergmeier et al. 2017; Cobo and Kocot 2021). Even so, there is substantial external uniformity among groups that, on the contrary, show great variability in terms of internal anatomical characters. This is especially the case among some families and genera of the order 'Cavibelonia' Salvini-Plawen, 1978 (recovered as non-monophyletic by Kocot et al. 2019).

Recent publications on solenogaster morphology and taxonomy have utilised both traditional and modern techniques. Micro-computed tomography is a promising technique for advancing aplacophoran taxonomy as this is a non-destructive method that can be used to obtain data on internal anatomy and three-dimensional (3-D) reconstructions. High levels of detail can be obtained for many anatomical structures but this is costly and advances in this technique are still required to improve the resolution needed to study small animals (Martínez-Sanjuán et al. 2022). In the same way, 3-D reconstructions based on histology (e.g. Bergmeier et al. 2016; Ostermair et al. 2018; Pedrouzo et al. 2019) provide information on the internal organs that is not available with standard manual reconstructions but this is a very time-consuming method. The combination of the study of the scleritome and DNA barcodes has been shown to allow a tentative identification of specimens, albeit at the family level in some cases, without the need for time-consuming or expensive techniques, improving the ability to estimate the number of lineages in a collection (e.g. Bergmeier et al. 2017, 2019). Nevertheless, although the study of sclerites and DNA barcodes can hasten the identification process, taxonomic expertise and histology are still needed for confident identification of specimens and are imperative for the description of new species.

In addition to these methodological difficulties, most solenogaster species seem to be rare. Most species are known only from the type locality and descriptions of many species are based on one or very few specimens (García-Álvarez and Salvini-Plawen 2007; Todt 2013). Moreover, most species are known from restricted areas; usually those in which a specific study has been dedicated or areas close to research centres with experts on the group (Todt 2013; García-Álvarez et al. 2014). Although new species are still found in reasonably well-studied areas (e.g. Kocot and Todt 2014; Pedrouzo et al. 2014), most species discovered in recent years come from remote or unexplored localities (e.g. Gil-Mansilla et al. 2008a, 2009; Bergmeier et al. 2017, 2019; Zamarro et al. 2019; Cobo and Kocot 2020) from where most of the existing species are considered to be new to science (Mora et al. 2011; M. C. Cobo and K. M. Kocot, pers. obs.).

The South China Sea (West Pacific Ocean) is one such area from which no solenogasters have been described to date. Our integrative taxonomic study of eight specimens collected during the DongSha 2014 and ZhongSha 2015 expeditions (led by the Muséum National d'Histoire Naturelle, Paris) in this region revealed four new species of Proneomeniidae Simroth, 1893: Proneomenia franziae sp. nov., Proneomenia satiata sp. nov., Proneomenia occulta sp. nov. and Dorymenia boucheti sp. nov. Traditionally solenogasters (Solenogastres sensu Salvini-Plawen, 1978) are classified in four orders and 24 families, based mainly on characteristics related to the cuticle (thickness and scleritome), radula, foregut glands and reproductive organs (García-Álvarez and Salvini-Plawen 2007; Kocot et al. 2019). The family Proneomeniidae Simroth, 1893 (order 'Cavibelonia') is characterised by a thick cuticle (>50 µm) with epidermal papillae and hollow acicular sclerites inserted in several layers, a polystichous radula, foregut glands of type-C (García-Álvarez and Salvini-Plawen 2007)-Epimeniatype (Handl and Todt 2005) and at least one pair of seminal receptacles (García-Álvarez and Salvini-Plawen 2007; García-Álvarez et al. 2009). This family includes 39 species (not including the new ones reported here) divided into 2 genera, Proneomenia Hubrecht, 1880 and Dorymenia Heath, 1911, that are distinguishable only by the presence of copulatory stylets in Dorymenia (García-Álvarez et al. 2009). The description and classification of the species examined here were reasonably straightforward following the established taxonomy. However, a phylogenetic analysis of molecular data obtained from the South China Sea samples, together with additional data from other proneomeniids collected from waters off Antarctica and Iceland, revealed that the monophyly of this apparently well-defined family is doubtful. Therefore we conducted ancestral character state reconstruction analyses to objectively evaluate the purported diagnostic characters of the family.

## Materials and methods

## **Species identification**

This work reports the study of eight specimens (loan of the Muséum National d'Histoire Naturelle, Paris) from the South

China Sea (West Pacific Ocean), collected during the DongSha 2014 and ZhongSha 2015 expeditions (project TF-DeepEvo) at depths between 232 and 1666 m (Table 1). Sampling was conducted in accordance with all local regulations and all expeditions operated under the regulations in force at the time in the countries and regions in question.

Following standard practices in solenogaster taxonomy (Bergmeier et al. 2017), specimens were examined using an integrative approach that combines both morphological techniques and DNA barcoding. This approach was implemented through the following workflow that permits the acquisition of all the necessary information to identify or describe specimens and generate DNA barcodes from the same animal.

# Sorting into morphospecies

Specimens were classified into morphospecies based on habitus and examination of mantle sclerites. External morphology was observed and photographed using an Olympus SZX-16 dissecting microscope and imaged with an Olympus SC50 camera. Larger animals (MNHN-IM-2013-61611 and MNHN-IM-2013-66993) were photographed using a Canon EOS 7D camera with a Cognisys StackShot automated macro focusing rail. Sclerites of all the animals were dislodged with a thin needle onto a slide with distilled water, air-dried and mounted with araldite or DEPEX mounting medium (Electron Microscopy Science). Sclerite preparations were observed under a Nikon Eclipse E200 light microscope and imaged with an iPhone 11 using a PhoneSkope smartphone optics adapter.

## Selection of specimens

At least one specimen of each morphospecies was selected for detailed study and cut in three parts (anterior, central and posterior regions).

## Study of the sclerites

The central region of each of the selected specimens (six specimens in total; Table 1) was imaged under a low-vacuum, low-accelerating voltage scanning electron microscope (Phenom Pro SEM). This enables the acquisition of ultrastructure-level data on the mantle sclerites and subsequent extraction of high quality DNA from the same sample as no post fixation or critical point drying is required.

# **DNA** barcoding

After study under the SEM, the central regions of the selected specimens were used to obtain 16S and COI barcodes. DNA was extracted using the EZNA MicroElute Genomic DNA Kit (Omega Bio-Tek) following the manufacturer's protocol except that  $20\,\mu\text{L}$  of OB-Protease was used. DNA concentration was measured using a NanoDrop Lite (Thermo). PCR amplification of fragments of the

mitochondrial 16S rRNA (LSU) gene and cytochrome c-oxioxidase subunit I gene (COI) were performed using Hot Start Taq 2× Master Mix (AMRESCO) following the manufacturer's instructions. For 16S, the solenogasterspecific primers 16Soleno-r and -f (Bergmeier et al. 2017) were used with the following cycling parameters: 2 min at 95°C, (5 s at 98°C, 5 s at 50°C and 20 s at 72°C)  $\times$  40 cycles, 1 min at 72°C and finally cooling at 10°C. For COI, the primers LCO Apl (TTTCTACTAAYCATAARGATATTGG) HCO2198 (TAAACTTCAGGGTGACCAAAAAATCA; Folmer et al. 1994) were used with the following cycling parameters: 2 min at 95°C, (20 s at 95°C, 15 s at 52°C and 30 s at  $72^{\circ}$ C) × 40 cycles, 7 min at  $72^{\circ}$ C and finally cooling at 10°C. PCR success was determined with gel electrophoresis using  $1 \times SB$  buffer at 120 V for 20 min. Products were either directly purified using the Omega Bio-tek EZNA Cycle Pure Quick kit and eluted in 25 μL of elution buffer or were gel-purified using the Omega Bio-Tek MicroElute Gel Extraction kit and eluted in 30 µL of elution buffer. Sanger sequencing was performed by GeneWiz and consensus sequences were assembled from forward and reverse reads using Sequencher. Sequences were successfully obtained from all samples except for 16S from MNHN-IM-2016-66989 (Table 1).

# Study of internal anatomy

The anterior and posterior regions of five of the specimens (Table 1) that contain the most taxonomically infomative structures were used for histology. One specimen (MNHN-IM-2013-61611) and the posterior region of another one (MNHN-IM-2013-66992) were sectioned using the protocol from McCutcheon et al. (2022) and stained using a combination of Weigert Hematoxylin and Gomori's Trichrome. All others were sectioned following the protocol from Cobo and Kocot (2020) that is based on Gil-Mansilla et al. (2008b) and uses Mallory's trichrome stain. In both cases, sections of 5 µm were obtained with a Leica RM2125 rotary microtome. Lateral reconstructions of the specimens were obtained by analysing the structures among the transverse histological sections (observed under a Nikon Eclipse E200 light microscope). Sections were photographed with an iPhone 11 using a PhoneSkope smartphone optics adapter. In addition, histology (following the protocol described in Cobo and Kocot 2020) of the anterior and posterior regions of six additional Proneomeniidae specimens included in the phylogenetic analysis (Table 1) was conducted. For three of these specimens, decalcification of the mantle sclerites was undertaken using hydrochloric acid instead of EDTA. This resulted in lower quality of the sections, some of which were overstained and this made study difficult. However, characterising the most relevant characters such as presence or absence of copulatory stylets, type of radula (but not always the number of teeth per row) and type of ventrolateral foregut glands remained possible. The sclerites of these species were

Table I. Specimens examined.

Collection number	Identification		Expedition	Station	Locality	Depth (m)	Sclerites		165	COI	Histology
(collector number)							LM	SEM			
MNHN-IM-2013-61955	Proneomenia franziae sp. nov.	Н	ZhongSha 2015	CP4148	16°07′N; 114°19′E	218–281	×	×	×	×	×
MNHN-IM-2013-66993	Proneomenia franziae sp. nov.	PΙ	ZhongSha 2015	CP4146	16°09′N, 114°16′E	232–314	×	×	×	×	_
MNHN-IM-2013-66989	Proneomenia franziae sp. nov.	P2	ZhongSha 2015	CP4148	16°07′N, 114°19′E	218–281	×	×	×	-	×
MNHN-IM-2013-61905	Proneomenia franziae sp. nov.	Р3	ZhongSha 2015	CP4146	16°09′N, 114°16′E	232–314	×	-	_	-	_
MNHN-IM-2013-66991	Proneomenia franziae sp. nov.	P4	ZhongSha 2015	CP4146	16°09′N, 114°16′E	232–314	×	-	_	-	-
MNHN-IM-2013-66992	Proneomenia occulta sp. nov.	Н	DongSha 2014	CP4123	21°36′N, 118°16′E	1612–1666	×	×	×	×	×
MNHN-IM-2013-61611	Proneomenia satiata sp. nov.	Н	ZhongSha 2015	CP4133	19°59′N, 116°24′E	999–1071	×	×	×	×	×
MNHN-IM-2013-50092	Dorymenia boucheti sp. nov.	Н	DongSha 2014	CP4123	21°36′N, 118°16′E	1612–1666	×	×	×	×	×
ALMNH:Inv:24164 (Ap262.2E)	Dorymenia sp.	-	LMG 13-12	П	63°56′06.7″S, 56°34′13.9″W	394	×	×	×	×	×
ALMNH:Inv:24159 (Ap232.2E)	Dorymenia sp.	-	NBP 12-10	23	76°14′42.9″S, 174°30′14.8″E	604	×	×	×	×	×
ALMNH:Inv:24160 (Ap271.2E)	Dorymenia sp.	-	LMG 13-12	18	63°23′19.0″S, 60°07′12.4″W	228	×	×	×	×	×
ALMNH:Inv:24162 (Ap218.2E)	Dorymenia sp.	-	NBP 20-10	17	75°19'46.7"S, 176°59'06.3"W	570	×	×	×	×	×
ALMNH:lnv:24165 (Ap214.2E)	Proneomenia sp.	-	NBP 12-10	14	73°29′54.7″S, 129°35′07.6″W	516	×	×	×	×	×
ALMNH:Inv:24161 (Ap205.2E)	Proneomenia gerlachei	-	NBP 12-10	10	72°10′38.9″S, 103°30′50.9″W	341	×	×	×	×	×
ALMNH:Inv:24163 (Ap206.2E)	Proneomenia sp.	-	NBP 12-10	ЮЬ	72°12′15.2″S, 103°35′46.8″W	612	×	×	×	×	×
MNHN-IM-2019-18270	Anamenia gorgonophila	_	Corsicabenthos 3	CR150	42°14′11.1″N, 008°31′54.06″E	50	×	×	×	×	×
	Dorymenia sarsii	-	Collected near Bergen, Norway		-		-	-	×	×	-

Type material of the new species from the South China Sea is deposited in the Muséum National d'Histoire Naturelle (MNHN) with the numbers included here. Specimens from Antarctic cruises have been deposited at the Alabama Museum of Natural History (ALMNH) and are listed with ALMNH catalogue number and collector number (e.g. Ap262.2E). ×, data obtained; H, holotype; P, paratype; LM, light microscopy.

also studied under SEM and compound light microscopy as described above.

# **Species descriptions**

The new species were described based on morphological data. Ecological information that was available was also considered. The proposed names were registered in ZooBank and barcode sequences were deposited in the Nucleotide database in GenBank (Table 2).

# Phylogenetic analysis and species delimitation

A phylogenetic analysis was conducted to confirm the identification of the new species within each genus and to examine the validity of the family Proneomeniidae. In addition to the 16S and COI barcodes obtained, sequences from 11 other Proneomeniidae species and 7 other species thought to be closely related to Proneomeniidae were included in the analysis (Table 2). Selection of the related taxa and outgroups was based on the results of Kocot et al. (2019) and our own unpublished DNA barcode data. Two solenogaster species of the order Pholidoskepia (Wirenia argentea Odhner, 1921 and Gymnomenia pellucida Odhner, 1921) were selected as the outgroup (Table 2). Sequences for each gene were aligned with MAFFT (ver. 7.487, https://www.ebi.ac.uk/Tools/msa/mafft/; Katoh and Standley 2013) and concatenated into a supermatrix. Sequences were partitioned by gene and for COI, by codon position. A consensus tree was produced using maximum likelihood with the best fitting model for each partition with 1000 rapid bootstraps in IQ-TREE2 (ver. 2.1.3, see https:// github.com/iqtree/iqtree2; Minh et al. 2020).

Species delimitation was performed on the concatenated dataset using Assemble Species by Automatic Partitioning (ASAP) with simple distance and default parameters on the ASAP web server (https://bioinfo.mnhn.fr/abi/public/asap/asapweb.html, accessed 5 March 2023; Puillandre et al. 2021).

#### Ancestral character state reconstruction

In light of the reconstructed phylogeny, we assessed the evolution of nine key traits commonly used for delineating solenogaster taxonomic groups: body size, general habitus, radula, ventrolateral foregut glands, seminal receptacles, respiratory folds, copulatory stylets, dorsoterminal sensory organs and abdominal spicules (Supplementary Table S1; data available from FigShare). Body size was divided into three categories: small (1–20 mm), medium (20–100 mm) and large (>100 mm). To characterise the general habitus, we followed the works of Salvini-Plawen (1985, 2003) where this is described as smooth, rough or shaggy. Animals with smooth habitus are those where most of the sclerites are scales and therefore the body surface has a velvety or scaly aspect. The rough habitus is characteristic of animals with a thick cover of acicular sclerites mostly

embedded in the cuticle. Shaggy animals are those in which the acicular sclerites protrude from the cuticle. Radula and ventrolateral foregut glands were analysed with two different coding schemes and the radula was in turn analysed under two different coding schemes. The first analysis of the radula was based on the classification in García-Álvarez and Salvini-Plawen (2007) with five categories. In the second analysis, these five types were reduced to four: the radula types distinguished previously as 'pectinate' and 'biserial' were grouped within the 'distichous' radula type. This distinct classification system is based on our observations and the literature (Salvini-Plawen 1997; Scheltema et al. 2003; Saito and Salvini-Plawen 2010). Similarly, the ventrolateral foregut glands were analysed under two different coding schemes. The first analysis of the ventrolateral foregut glands followed the classification of Salvini-Plawen (1978) for these organs whereas the second one followed the classification of Handl and Todt (2005). The seminal receptacles were initially coded as present or absent but these are present in all the species considered except for Dorymenia boucheti sp. nov. Due to the importance in the traditional taxonomy of Solenogastres (García-Álvarez and Salvini-Plawen 2007), we also coded this as follows: lack of seminal receptacles, bundles of one to four seminal receptacles and bundles of more than four seminal receptacles. This distinction is based on the common use of these numbers in the description of species within these groups. The remaining characters, including respiratory folds, copulatory stylets, dorsoterminal sensory organ(s) and abdominal spicules were coded as present or absent. Morphological data were put into a comma separated value (csv) file (available from FigShare) and mapped onto the ML consensus tree using Phytools (ver. 1.0-3, see https://cran.r-project.org/ package = phytools/; Revell 2012) as implemented through R (ver. 4.2.0, R Foundation for Statistical Computing, Vienna, Austria, see https://www.R-project.org/) on the University of Alabama High-Performance Computing cluster (UAHPC). Model optimisations were analysed using the fitMk function in Phytools that fits the Mk model (Lewis 2001) to the phylogenetic tree and a discrete character state matrix under the equal rates (ER), symmetric rates (SYM) or all rates different (ARD) reversible models. For binary characters, only ER and ARD models were compared because the SYM model is equal to ER when only two character states are present. The best model was selected by a comparison of Akaike information criterion (AIC) scores. ARD was the best-fitting model for DSO and respiratory folds whereas ER was the best-fitting model for all the other traits. The make.simmap function in Phytools was used in parallel to stochastically map character states with a resulting total of 100 000 simulations. For binary characters (abdominal spicules, copulatory stylets, DSO and respiratory folds), density maps were constructed using the densityMap function in Phytools.

Table 2. Sequences considered for the analysis with corresponding GenBank numbers, references and identification.

Name in the tree	Voucher number	Family	GenBank number (16S)	GenBank number (COI)	Reference
Anamenia gorgonophila	MNHN-IM-2019-18270	Strophomeniidae	OQ600030	OQ597876	Present work
Dorymenia boucheti sp. nov.	MNHN-IM-2013-50092*	Proneomeniidae	OQ600025	OQ597881	Present work
Dorymenia sarsii	n/a	Proneomeniidae	OQ600024	OQ597883	Present work
Dorymenia sp.	ALMNH:Inv:24164*	Proneomeniidae	OQ600022	OQ597885	Present work
Dorymenia sp.	ALMNH:Inv:24162*	Proneomeniidae	OQ600020	OQ597887	Present work
Dorymenia sp.	ALMNH:Inv:24160*	Proneomeniidae	OQ600018	OQ597889	Present work
Dorymenia sp.	ALMNH:Inv:24159*	Proneomeniidae	OQ600017	OQ597890	Present work
Dorymenia tricarinata	Ap231.5R	Proneomeniidae	OQ618431	OQ600547	Present work
Epimenia autralis	MCZ DNA100841	Epimeniidae	AY377614	AY377722	Okusu et al. (2003)
Epimenia babai	MCZ DNA100843	Epimeniidae	AY377616	AY377724	Okusu et al. (2003)
Gymnomenia pellucida	BioSample:SAMN06141848	Gymnomeniidae	OQ618433	OQ600550	Present work
Hypomenia sanjuanensis	Ap183.1R	Pruvotinidae	OQ618434	OQ600549	Present work
Kruppomenia genslerae	ZSM Mol 20170348	Simrothiellidae	MG603271	MN531184	Ostermair et al. (2018)
Proneomenia custodiens	ZMBN 94109	Proneomeniidae	OQ618430	KJ568518	Present work, Kocot and Todt (2014)
Proneomenia franziae sp. nov.	MNHN-IM-2013-61955*	Proneomeniidae	OQ600027	OQ597879	Present work
Proneomenia franziae sp. nov.	MNHN-IM-2013-66993	Proneomeniidae	OQ600029	OQ597877	Present work
Proneomenia franziae sp. nov.	MNHN-IM-2013-66989*	Proneomeniidae	-	OQ597882	Present work
Proneomenia gerlachei	ALMNH:Inv:24161*	Proneomeniidae	OQ600019	OQ597888	Present work
Proneomenia occulta sp. nov.	MNHN-IM-2013-66992*	Proneomeniidae	OQ600028	OQ597878	Present work
Proneomenia satiata sp. nov.	MNHN-IM-2013-61611*	Proneomeniidae	OQ600026	OQ597880	Present work
Proneomenia sluiteri	ZMBN 94113	Proneomeniidae	OQ618429	KJ568517	Present work, Kocot and Todt (2014)
Proneomenia sp.	ALMNH:Inv:24165*	Proneomeniidae	OQ600023	OQ597884	Present work
Proneomenia sp.	ALMNH:Inv:24163*	Proneomeniidae	OQ600021	OQ597886	Present work
Simrothiella margaritacea	Ap189.1R	Simrothiellidae	OQ618432	OQ600548	Present work
Unciherpia hirsuta	MNHN-IM-2019-18279	Pruvotinidae	OQ600031	OQ597875	Present work
Wirenia argentea	n/a	Gymnomeniidae	MG855856	MG855759	Mikkelsen et al. (2018)

Voucher numbers: ALMNH, Alabama Museum of Natural History, Tuscaloosa, AL, USA; Ap, reference number of vouchers from Kocot et al. (2019); BioSample, from De Oliveira et al. (2016); MNHN, Muséum national d'Histoire naturelle, Paris, France; MCZ, Museum of Comparative Zoology, Harvard University, Cambridge, MA, USA; ZMBN, Museum of Zoology at the University of Berge, Norway; ZSM, Zoologische Staatssammlung München (the Bavarian State Zoological Collections), Munich, Germany. Vouchers with an asterisk (\*) are histological sections and sclerites preparations that were obtained and studied for the present work.

# **Taxonomy**

# Family **PRONEOMENIIDAE** Simroth, 1893

## Genus Proneomenia Hubrecht, 1880

Type species: Proneomenia sluiteri Hubrecht, 1880.

Species included: *P. acuminata* Wirén, 1892; *P. bulbosa* García-Álvarez, Zamarro & Urgorri, 2009; *P. custodiens* Todt & Kocot, 2014; *P. desiderata* Kowalevsky & Marion, 1887; *P. epibionta* Salvini-Plawen,

1978; *P. gerlachei* Pelseneer, 1901; *P. hawaiiensis* Heath, 1905; *P. insularis* Heath, 1911; *P. praedatoria* Salvini-Plawen, 1978; *P. sluiteri* Hubrecht, 1880; *P. stillerythrocytica* Salvini-Plawen, 1978; *P. valdiviae* Thiele, 1903.

## **Diagnosis**

Thick cuticle with epidermal papillae. Hollow acicular sclerites arranged in several layers. Polystichous radula. Foregut glands of type-C–*Epimenia*-type. Midgut with constrictions. With at least one pair of seminal receptacles. Secondary

genital opening unpaired. Without copulatory stylets. With dorsoterminal sense organ(s). Without respiratory folds.

# Proneomenia franziae Cobo & Kocot, sp. nov.

(Fig. 1a, 2a, 3a, 4a, b, 5.)

ZooBank: urn:lsid:zoobank.org:act:01B8766D-C45A-4D73-BA75-C1948 EE3AFD5

# Type material

**Holotype.** MNHN-IM-2013-61955 in serial sections of the anterior and posterior region (38 slides, 5  $\mu$ m), fragment of the central region preserved in 96% ethanol, light microscopy preparations of the sclerites (3 slides), DNA barcodes (GenBank: OQ600027; OQ597879); South China Sea, ZhongSha 2015 expedition station CP4148, 218–281-m depth. Type series deposited at the Muséum National d'Histoire Naturelle, Paris (MNHN).

**Paratype 1.** MNHN-IM-2013-66993 preserved in 96% ethanol, light microscopy preparations of the sclerites (3 slides), SEM preparations of sclerites (1 stub), DNA barcodes (GenBank: OQ600029; OQ597877); South China Sea, ZhongSha 2015 expedition station CP4146, 232–314-m depth.

Paratype 2. MNHN-IM-2013-66989 in serial sections of the anterior and posterior region (49 slides,  $5\,\mu m$ ), fragment of the central region preserved in 96% ethanol, light microscopy preparations of the sclerites (3 slides), DNA barcodes (GenBank: OQ597882); same locality as MNHN-IM-2013-61955.

**Paratype 3.** MNHN-IM-2013-61905, preserved in 96% ethanol, light microscopy preparations of the sclerites (3 slides); same locality as MNHN-IM-2013-66693.

**Paratype 4.** MNHN-IM-2013-66991 preserved in 96% ethanol, light microscopy preparations of the sclerites (3 slides); same locality as MNHN-IM-2013-66993.

#### **Diagnosis**

Elongate animal (30–40 mm long and 2–3 mm wide) without keels or dorsal protuberances. With a small finger-like projection at the posterior end. Light cream to white in 96% ethanol. Pedal groove externally evident. Thick cuticle with straight and curved hollow acicular sclerites. Polystichous radula with 30–32 uniform teeth per row, with a posterior double radular sac. Atrium with numerous (30–50) long, single (= unbranched) papillae. Without copulatory stylets or abdominal spicules. Two pairs of seminal receptacles. With a dorsoterminal sensory organ.

## **Distribution**

South China Sea (Pacific Ocean) (ZhongSha 2015; station CP4148, 16°07′N–114°19′E; station CP4146, 16°09′N–114°16′E; 218–314-m depth).

## **Etymology**

Female genitive in honour of Dr Franziska Bergmeier, an expert in solenogaster taxonomy, for valuable comments

and help that led to the description of this new species and for her friendship.

# **Description**

Measurements of the internal characters and reconstruction (Fig. 4a, b) based on the holotype (MNHN-IM-2013-61955) and paratype 2 (MNHN-IM-2013-66989); habitus and sclerites based on the five available specimens.

#### **Habitus**

Elongate animal (30–40 mm long and 2–3 mm wide), rounded in cross-section (Fig. 1*a*). With a rounded anterior end with a small distal protuberance (Fig. 1*a*1) and with a small finger-like projection at the posterior end, preceded by a widening of the body (Fig. 1*a*2–*a*4). Pedal groove marked externally. Light cream to white in 96% ethanol (Fig. 1*a*).

#### **Mantle**

Thick cuticle ( $100-200\,\mu m$  dorsal,  $100-150\,\mu m$  ventral), in which hollow acicular sclerites are inserted in several layers. With epidermal papillae. The sclerites have a wide range of sizes. Most of the hollow acicular sclerites are straight ( $100-500\,\mu m$  long,  $15-30\,\mu m$  wide) (Fig. 2a4, 3a1-a3), although some have a more marked curvature at the proximal end (Fig. 3a4), with the internal cavity along most of the length of the sclerite ( $100-500\,\mu m$  long,  $20-30\,\mu m$  wide) (Fig. 2a4, 3a1, a2, a4). Some sclerites are also remarkably small, ( $100-120\,\mu m$  long,  $10\,\mu m$  wide) (Fig. 3a3). The sclerites along the pedal groove have a characteristic arrangement. Inserted between hollow straight acicular sclerites there are knife-shaped scales with a marked keel ( $120-160\,\mu m$  long,  $10-20\,\mu m$  wide) (Fig. 2a2) and solid, flat leaf-shaped scales ( $120-140\,\mu m$  long,  $20\,\mu m$  wide) (Fig. 2a3).

#### Pedal groove and pallial cavity

The pedal pit (300 µm long, 15 µm wide, 250–400 µm high) is strongly ciliated. The anterior pedal glands connect with the dorsal wall of the pedal pit (Fig. 5c). These are very voluminous ventrally and extend towards the dorsal region of the body. The pedal pit gives rise to three triangular pedal folds (Fig. 5d, f). In the central region of the body the lateral folds become smaller (20 µm wide, 30 µm high) and lap the medial triangular fold (70 µm wide, 80–100 µm high); this is maintained until entering the pallial cavity. The pallial cavity opens ventrally (1050 µm long, 100–400 to µm wide, 50–625 µm high) (Fig. 4b). The rectum opens into the pallial (=mantle) cavity dorsally with the spawning ducts (fused to a single tube) opening into the central region of the cavity as a sphincter (Fig. 4b). With a ciliated and folded pallial cavity wall (Fig. 5h).

#### Digestive system

The mouth opens dorsally at the posterior end of the atrium. The foregut is slightly wider in the anterior region



Fig. 1. Habitus of Proneomeniidae species from the South China Sea. (a) Proneomenia franziae sp. nov. (a1) Detail of the anterior end. (a2–a4) Detail of the finger-like posterior in different specimens. (b) Proneomenia satiata sp. nov. (b1) Detail of the finger-like posterior projection. (b2) Detail of the anterior end. (c) Proneomenia occulta sp. nov. (d) Dorymenia boucheti sp. nov. The star indicates the anterior region.

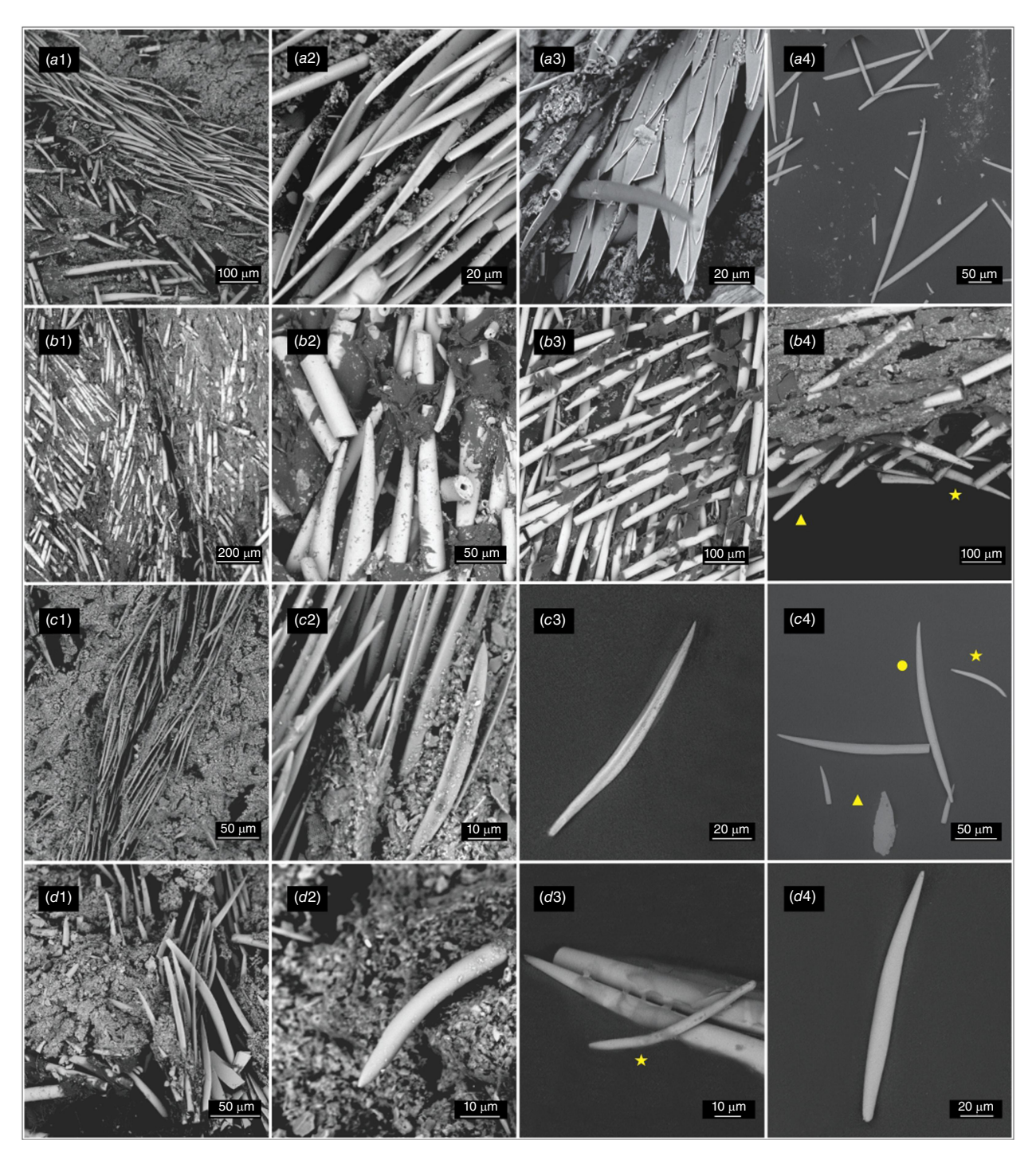


Fig. 2. Sclerites of Proneomeniidae from the South China Sea (SEM images). (a) Proneomenia sp. nov.: (a1) Detail of the pedal groove; (a2) detail of the arrangement of the sclerites in the pedal groove; (a3) detail of the scales of the pedal groove; (a4) isolated hollow acicular sclerites. (b) Proneomenia satiata sp. nov.: (b1) detail of the pedal groove; (b2) detail of the tips of the dorsal hollow acicular sclerites; (b3) arrangement of the dorsal acicular sclerites; (b4) detail of the tips (star) and proximal end (triangle) of the dorsal hollow acicular sclerites. (c) Proneomenia occulta sp. nov.: (c1) detail of the pedal groove; (c2) detail of the arrangement of the sclerites in the pedal groove; (c3) knife-shaped scale of the pedal groove; (c4) isolated sclerites showing pallet-shaped sclerites (star), hollow acicular sclerite (circle) and leaf-shaped scale (triangle). (d) Dorymenia boucheti sp. nov.: (d1) detail of the arrangement of the sclerites in the pedal groove; (d2) tip of a curved hollow acicular sclerite; (d3) hollow straight acicular sclerites and a pallet-shaped sclerite (star); (d4) isolated hollow acicular sclerite.

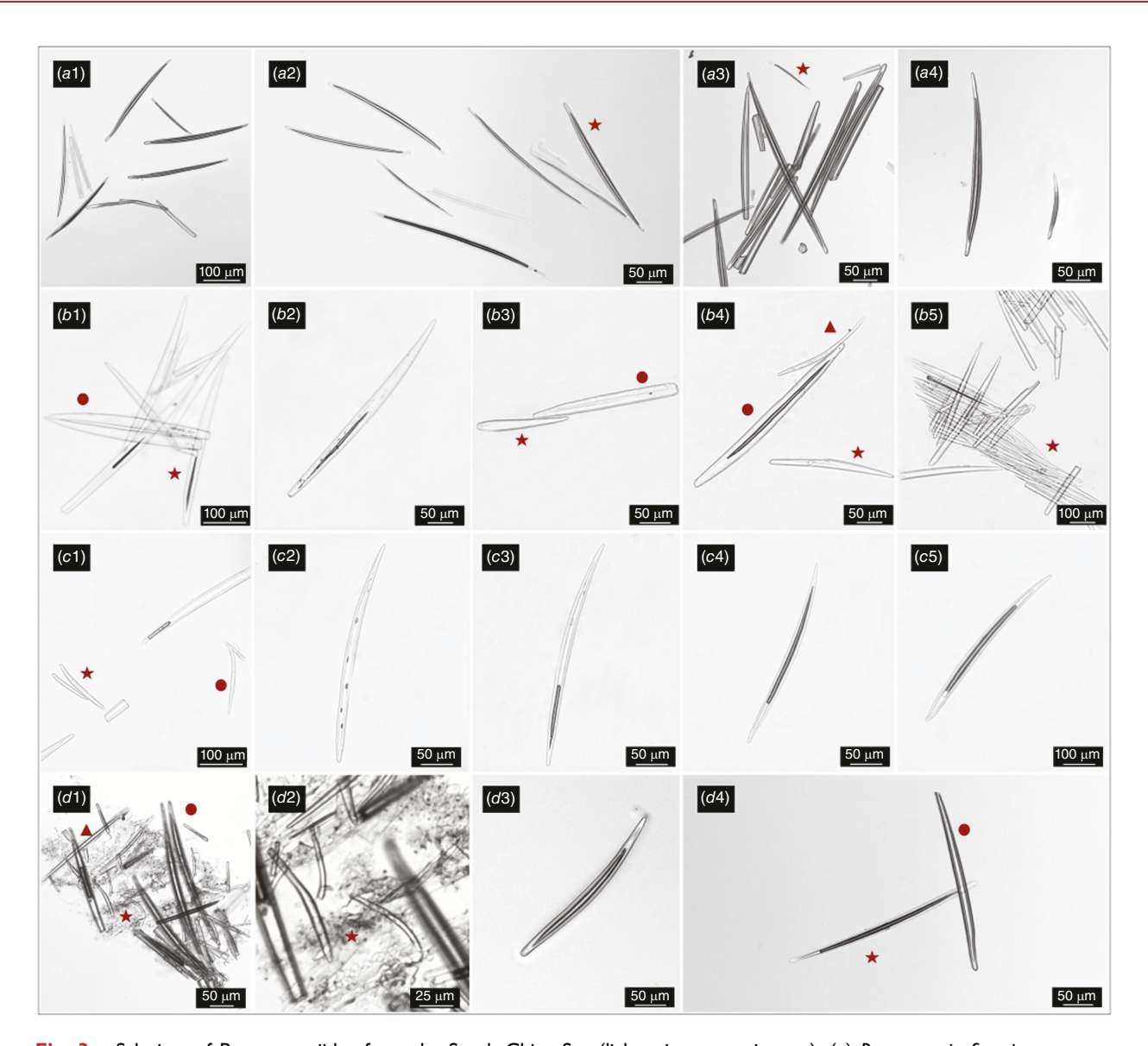


Fig. 3. Sclerites of Proneomeniidae from the South China Sea (light microscopy images). (a) Proneomenia franziae sp. nov.: (a1) straight hollow acicular sclerites with a curvature at the proximal end; (a2) long straight hollow acicular sclerites and straight hollow acicular sclerites with a curvature at the proximal end (star); (a3) several hollow acicular sclerites and curved small hollow acicular sclerites with the internal cavity not in the proximal region (star); (a4) two sizes of straight hollow acicular sclerites with a curvature in the proximal end. (b) Proneomenia satiata sp. nov.: (b1) hollow acicular sclerites, slightly curved sclerites with a truncated proximal end and pointed distal end (circle), hollow slightly curved acicular sclerites with a curvature at the proximal rounded end (star); (b2) hollow slightly curved sclerites with a truncated proximal end and pointed distal end; (b3) hollow short acicular sclerites with a small internal cavity only in the base of the sclerite (star), hollow straight acicular sclerites with a truncated proximal end (circle); (b4) hollow slightly curved sclerites with a truncated proximal end and pointed distal end (circle), small hollow slightly curved sclerites with a truncated proximal end (star), small curved hollow acicular sclerites (triangle); (b5) fragments of hollow acicular sclerites (star). Long straight hollow acicular sclerites. (c) Proneomenia occulta sp. nov.: (c1) small curved hollow acicular sclerites (star), pallet-shaped sclerite (circle); (c2) hollow acicular sclerites without a curvature at the proximal end; (c3-c5) hollow acicular sclerites with a curvature at the proximal end. (d) Dorymenia boucheti sp. nov.: (d1) hollow straight acicular sclerites (triangle), paddle-shaped sclerites (star), hollow curved acicular sclerites (circle); (d2) paddle-shaped sclerites (star); (d3) hollow curved acicular sclerites; (d4) straight hollow acicular sclerite (star), straight hollow acicular sclerite with a curvature at the proximal end (circle).

(275  $\mu$ m long, 220–400  $\mu$ m wide, 600–800  $\mu$ m high) and runs towards the dorsal region of the body. In this anterior region the foregut is highly glandular and there is a dorsal

glandular pouch (Fig. 5b). Thereafter the foregut runs almost parallel to the pedal groove as an oval to rounded tube (1350  $\mu$ m long, 120–600  $\mu$ m wide, 130–450  $\mu$ m high),

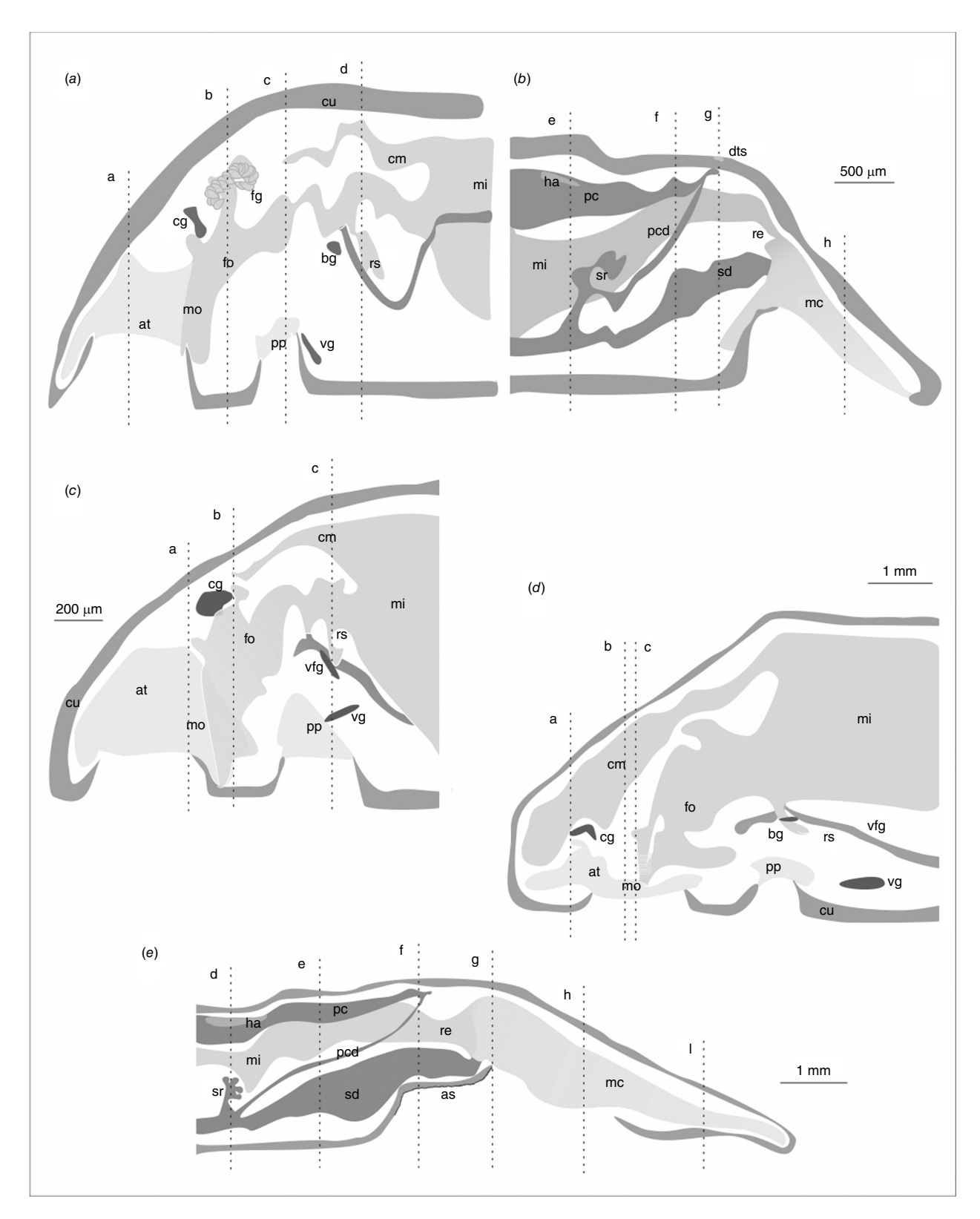


Fig. 4. (Caption on next page)

Fig. 4. Reconstructions of the internal anatomy of the new *Proneomenia* species. (a) Reconstruction of the anterior internal anatomy of *Proneomenia franziae* sp. nov. (a–d correspond with the serial sections of the holotype in Fig. 5). (b) Reconstruction of the posterior internal anatomy *Proneomenia franziae* sp. nov. (e–h correspond with the serial sections of the holotype in Fig. 5). (c) Reconstruction of the anterior internal anatomy of *Proneomenia occulta* sp. nov. (a–c correspond with the serial sections of the holotype in Fig. 6). (d) Reconstruction of the anterior internal anatomy of *Proneomenia satiata* sp. nov. (a–c correspond with the serial sections of the holotype in Fig. 7). (e) Reconstruction of the posterior internal anatomy of *Proneomenia satiata* sp. nov. (d–i correspond with the serial sections of the holotype in Fig. 7). at, atrium; as, abdominal spicules; bg, buccal ganglia; cg, cerebral ganglion; fg, pharyngeal glands; cm, midgut caecum; cs, copulatory stylets; cu, cuticle; dts, dorsoterminal sensory organ; fo, foregut; fg, foregut gland; ha, heart; mc, pallial cavity; mi, midgut; mo, mouth; pc, pericardium; pcd, pericardioduct; pf, pedal fold(s); pp, pedal pit; ra, radula; re, rectum; rs, radular sac; sd, spawning duct; sr, seminal receptacles; vg, ventral ganglia; vfg, ventrolateral foregut glands; vrs, ventral radular sac or subradular pouch.

glandular and with a thick layer of musculature  $(100-140 \,\mu\text{m})$  (Fig. 4a, section c; Fig. 5c). In the radular region, the foregut is remarkably straight (120 µm wide, 130 µm high) (Fig. 4a, section d; Fig. 5d). The radula is polystichous (Fig. 5d, d') with a posterior double radular sac (the radular sac is bilobed at the posterior region) (200  $\mu$ m long, 250–280  $\mu$ m wide, 200  $\mu$ m high) with 30–32 single teeth per row. The teeth have a small base (7.5 µm wide) and are straight and long (33-35 μm long, 7.5 μm wide at the base to  $2.5 \,\mu m$  at the tip) (Fig. 5d'). The ventrolateral foregut glands are of the type-C-Epimenia-type, the tubes are long with several loops. Some of the turns are directed towards the anterior region of the body and reach the central (pre-radular) region of the pharynx. The foregut connects with the midgut through an esophagus. The midgut has slight lateral constrictions. There is a small dorsal caecum (775 µm long, 200-450 µm wide, 25-200 µm high) (Fig. 4a). The rectum opens dorsally in the pallial cavity  $(200-300 \,\mu\text{m} \text{ wide}, 200-250 \,\mu\text{m high}) \,(\text{Fig. 4b}).$ 

#### Cerebral ganglion and sense organs

The cerebral ganglion (80 µm long, 150-350 µm wide, 80-160 µm high) is located dorsally to the posterior region of the atrium and the mouth. In the posterior part, the cerebral ganglion is bilobed. The atrium opens ventrally and gives way to a wide cavity (350 µm long, 400-600 µm wide, 400-470 µm high) with numerous (30-50) long, single (=unbranched) papillae (up to  $14 \mu m \log$ ) (Fig. 5a). In the central region of the atrium, a heavily ciliated protrusion of the dorsal epithelium rises and is divided into two folds or larger papillae (150 × 80 µm) and there are similar structures in the ventral region, in the atrial border (Fig. 4a, section a; Fig. 5a). This corresponds to the so-called atrial sensory organ or the atrium (Heath 1911; Salvini-Plawen 1978). With a cup-shaped dorsoterminal sensory organ (200 μm long, 120 μm wide, 80 μm high) (Fig. 4b, 5g, g') located in the posterior region, slightly anterior to the opening of the pallial cavity.

## Gonopericardial system

The gonads give rise to a pericardium (1035  $\mu m$  long reconstructed, 300–850  $\mu m$  wide, 200–600  $\mu m$  high) that has a significantly straight posterior region (~300  $\mu m$  in

length; 80 µm in diameter). The heart is restricted to the posterior half of the pericardium and attached to the dorsal wall (Fig. 5e). The pericardioducts (850 μm long, 50–100 μm wide 75-120 µm high) connect to the straight region of the pericardium (Fig. 4b, section g; Fig. 5g) and with the spawning ducts in their most posterior region, where there is a pair of globular seminal receptacles, with a posterior turn, attached to each of the pericardioducts (350 µm long, 70-250 µm wide, 50-100 µm high) (Fig. 4b, section e; Fig. 5e). The spawning ducts are paired at the origin (850 µm long, 250-600 µm wide, 150-800 µm high) (Fig. 4b, section e; Fig. 5e) and become a single large duct (Fig. 4b, section f; Fig. 5f) in the mid-region (750 μm long, 1200-1500 μm wide, 800-850 μm high) and open as a single duct through a sphincter (25-35 µm in diameter) in the central region of the pallial cavity. Without accessory copulatory structures.

## **Remarks**

Within Proneomeniidae (thick cuticle with epidermal papillae, hollow acicular sclerites in several layers, polystichous radula, type-C–*Epimenia*-type foregut glands and at least one pair of seminal receptacles), the specimens examined belong to *Proneomenia* as these lack copulatory spicules (García-Álvarez and Salvini-Plawen 2007; García-Álvarez *et al.* 2009). All of the 12 species in this genus (including the new species described here) are found at bathyal depths (between 200 and 1600 m) except for one (*P. desiderata*; collected in the Mediterranean Sea at 30-m depth). Therefore the depth range this species was collected from is consistent with that of most species of the genus (Tables 3, 4).

The animals studied lack dorsal keels or protuberances and have a marked posterior, tail-like digitiform projection that distinguishes these from *P. custodiens* that has a rounded posterior end and a slight keel in the posterior body region (Todt and Kocot 2014); *P. epibionta* and *P. stillerythrocytica*, both with a dorsal keel (Heath 1905; Salvini-Plawen 1978); and *P. praedatoria* that has seven protuberances (Heath 1905). Therefore, in view of the habitus these can be differentiated from four of the *Proneomenia* species. In addition, these have a remarkable dorsal foregut gland as those described for *P. acuminata*, *P. gerlachei*, *P. bulbosa*, *P. praedatoria*, *P. hawaiiensis* and *P. valdiviae* (Wirén 1892; Pelseneer 1901; Thiele 1903; Heath 1905;

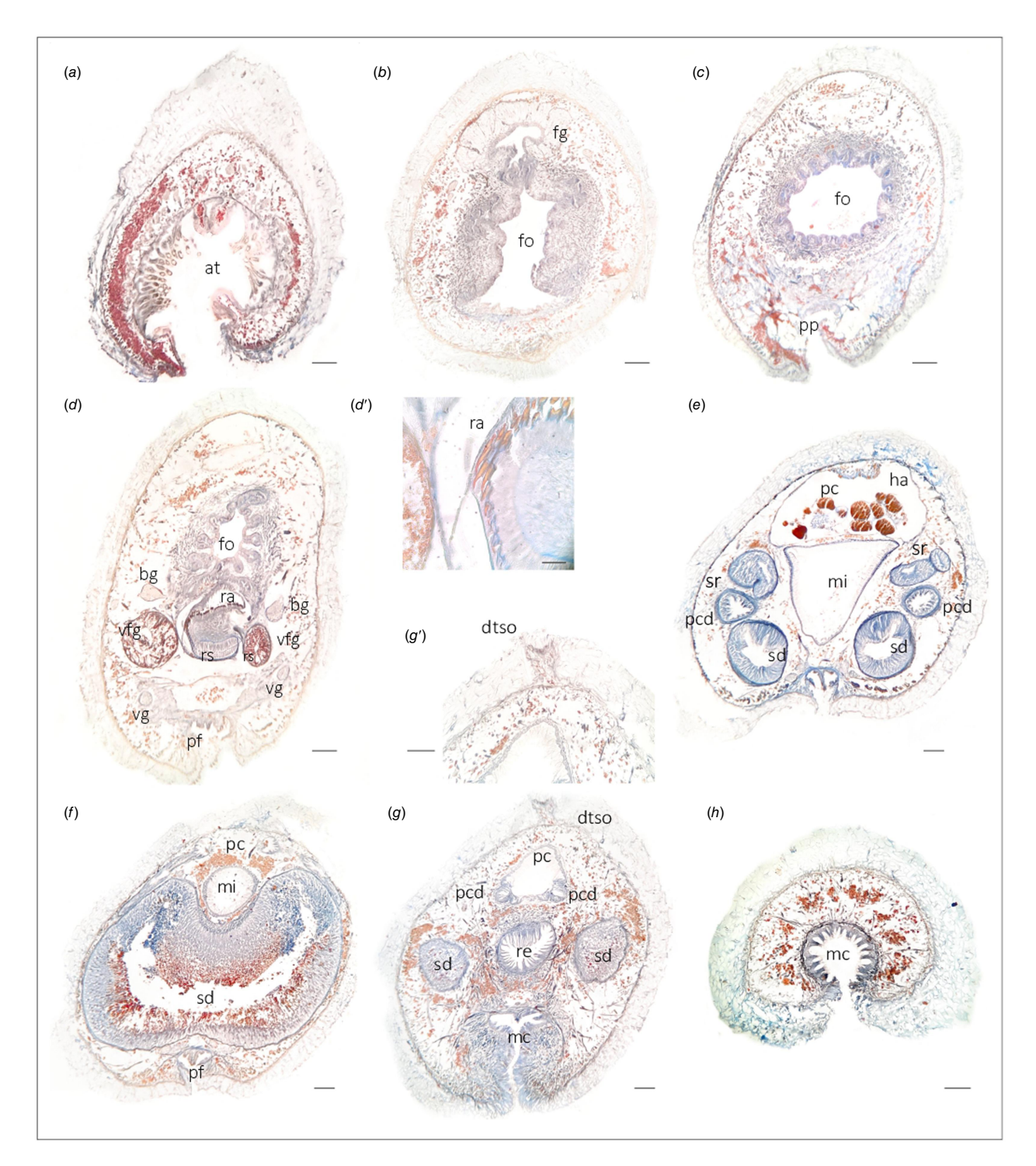


Fig. 5. Serial sections of the holotype of *Proneomenia franziae* sp. nov. Anterior (a-d) and posterior region (e-h). Abbreviations as per Fig. 4. Scale bars: a-d, e-g, g', h,  $100 \mu m$ ; d',  $10 \mu m$ .

Salvini-Plawen 1978; García-Álvarez et al. 2009) (Tables 3, 4). Therefore this character excludes the species *P. desiderata*, *P. sluiteri* and *P. insularis* (Hubrecht 1880; Kowalevsky and Marion 1887; Heath 1911). The radula of the new species (with 30–32 teeth per row) is different from that of *P. acuminata* (with 28 teeth), *P. gerlachei* (with

40 teeth), *P. bulbosa* (with 25 teeth), *P. praedatoria* (with 45 teeth), *P. hawaiiensis* (with 38–45 teeth) and *P. valdivia* (with 18 teeth) (Wirén 1892; Thiele 1903; Heath 1905; Salvini-Plawen 1978; García-Álvarez *et al.* 2009). Therefore, considering the external aspect and important internal characteristics (Tables 3, 4), the specimens examined here

Table 3. Distribution and morphological characteristics considered for the remarks of the *Proneomenia* species (data from the original descriptions: Hubrecht 1880, Kowalevsky and Marion 1887, Wirén 1892, Pelseneer 1901, Salvini-Plawen 1978, Todt and Kocot 2014).

	P. sluiteri Hubrecht, 1880	P. custodiens Todt & Kocot, 2014	P. acuminata Wirén, 1892	P. desiderata Kowalevsky & Marion, 1887	P. epibionta Salvini- Plawen, 1978	P. stillerythrocytica Salvini-Plawen, 1978	P. gerlachei Pelseneer, 1901
Distribution	NE Atlantic	NE Atlantic	NW Atlantic	Mediterranean	SW Atlantic	SW Atlantic	Antarctic
	Spitzbergen, Barents Sea, Kara Sea, Laptev Sea, Iceland	The Rose Garden	Florida, Martha's Vineyard	Marseille	Falkland Islands	Falkland Islands	Bellingshausen Sea
Depth (m)	45–300	284	250-650	20–30	646–845	512–586	550
Size (mm)	105-150 × 11-12	10 × 3.5	20-30 × 1.8	10 × ?	30 × 2	37 × 2	45 × 2.5
Dp	+	-	+	±	_	_	+
Keel/ridges	-	+ (slight posterior)	-	_	+	+ (slight)	-
Pedal fold	Several-I	3	I	3	I	?	?
Ap	Numerous slender	Numerous single and slender	?	Numerous single	Numerous single	Numerous single	Numerous single and trilobulated
Teeth per row	19–20	18–22	28	14	42–46	42–52	40->40
Fg	-	-	+	_	-	_	+
Esophagus	+	+	+	_	_		_
Dts	I	T	1	I	4	3	I
As	+	+	+	+	+	+	_
Sr	1	3	I	2	2	2	1

Ap, atrial papillae; As, abdominal spicules; Dp, posterior digitiform projection; Dts, dorsoterminal sensory organ; Fg, dorsal foregut gland; Sr, seminal receptacles; +, presence; -, absence; ?, no information.

Table 4. Distribution and morphological characteristics considered for the remarks of the *Proneomenia* species (data from the original descriptions: Thiele 1903, Heath 1905, Heath 1911, Salvini-Plawen 1978, García-Álvarez et al. 2009).

	P. bulbosa García- Álvarez, Zamarro & Urgorri, 2009	P. praedatoria Salvini- Plawen, 1978	P. valdiviae Thiele, 1903	P. hawaiiensis Heath, 1905	P. insularis Heath, 1911	P. franziae sp. nov.	P. occulta sp. nov.	P. satiata sp. nov.
Distribution	Antarctic	S Indian	S Indian	N Pacific	N Pacific	S Pacific	S Pacific	S Pacific
	Bellingshausen Sea (Antarctica)	Kerguelen Islands, Drake Strait	Zanzibar (East Africa)	Hawaii (Albatross St 3864)	Hawaii (Albatross St 4157)	South China Sea	South China Sea	South China Sea
Depth (m)	603	585-1240	748	270–330	1400-1800	218–314	1612–1666	999–1071
Size (mm)	43 × 25	28 × 2	37 × 2	36 × 2	?×1.5	30–40 × 2–3	17.5 × 2	20-35 × 1.5-1.8
Dp	+	_	+	+	?	+	+	+
Keel/ridges	-	7	_	-	-	_	_	_
Pedal fold	1	3	3	?	?	3	I	3
Ар	Numerous single	Single	Numerous	Numerous single	Numerous single, bilobulated and trilobulated	30–50 long single	24 single	Numerous small single
Teeth per row	22–25	45	18	38 <del>-4</del> 5	24	30–32	12	21–22
Fg	+	+	+	+	-	+	_	_
Esophagus	+	_		+	+	+	+	_
Dts	1	I <b>–</b> 2	I	1	?	_	?	1
As	-	?	_	?	?	_	_	+
Sr	2	1	2	I	?	2	?	4

Ap, atrial papillae; As, abdominal spicules; Dp, posterior digitiform projection; Dts, dorsoterminal sensory organ; Fg, dorsal foregut gland; Sr, seminal receptacles; +, presence; -, absence; ?, no information.

do not belong to any described species of *Proneomenia* and constitute a species new to science.

# Proneomenia occulta Cobo & Kocot, sp. nov.

(Fig. 1c, 2c, 3c, 4c, 6.)

ZooBank: urn:lsid:zoobank.org:act:C294F01D-940B-4B98-A9ED-E8E9B 456E8F4

# Type material

**Holotype.** MNHN-IM-2013-66992 in serial sections of the anterior and posterior region (26 slides, sections  $5\,\mu m$  thick), fragment of the central region preserved in 95% ethanol, light microscopy preparations of the sclerites (3 slides), SEM preparations of sclerites (1 stub), DNA barcodes (GenBank: OQ600028; OQ597878); South China Sea, DongSha 2014 expedition station CP4123, 1612–1666-m depth. Type series deposited at the Muséum National d'Histoire Naturelle, Paris (MNHN).

## **Diagnosis**

Robust animal (17.5 mm long and 2–2.5 mm wide) with rounded anterior end and a finger-like projection at the posterior end. Ochre in 96% ethanol. Slightly hairy appearance. Pedal groove, pedal pit and pallial cavity externally evident. Thick cuticle with straight and curved hollow acicular sclerites. Polystichous radula with 12–14 uniform teeth per row. Numerous small, single (unbranched) atrial papillae (more than 40) and four large papillae in the atrium. Without copulatory stylets or abdominal spicules. Single pair of seminal receptacles. Presence of dorsoterminal sensory organ unknown.

#### **Distribution**

South China Sea (Pacific Ocean) (DongSha 2014; station CP4123; 21°36′N–118°16′E; 1612–1666-m depth).

# **Etymology**

From Latin *occultus*, *occulta*, *occultum*, meaning hidden, or having been hidden. In allusion to the unexpected identification of the animal as *Proneomenia* due to the external resemblance with *Dorymenia boucheti* sp. nov.

# **Description**

#### Habitus

Robust animal (17.5 mm long and 2–2.5 mm wide) without keel or body protrusions. Rounded anterior end and a finger-like projection at the posterior end. Pedal groove marked externally. Ochre in 96% ethanol (Fig. 1c).

#### **Mantle**

Thick cuticle (60–100 µm), with epidermal papillae and three to four layers of hollow acicular sclerites. Small palletshaped sclerites (Fig. 2c4) and knife-shaped scales in the pedal groove also present (Fig. 2c4). The hollow acicular sclerites have a wide range of sizes and are of three types: (1) small, curved, hollow acicular sclerites (50–80 µm long, 8–10  $\mu$ m wide) (Fig. 3c1); (2) hollow acicular sclerites with a curvature at the proximal end, with the internal cavity along most of the length of the sclerite (250–350 µm long, 15-20 μm wide) (Fig. 2c4, 3c3-c5); (3) hollow acicular sclerites without a curvature at the proximal end, with the internal cavity along most of the length of the sclerite  $(300-350 \, \mu \text{m} \, \log, \, 20-30 \, \mu \text{m} \, \text{wide})$  (Fig. 3c2). The small pallet-shaped (oar-shaped or trowel-like) sclerites (80-100 μm long, 10 μm wide) (Fig. 2c4) are more abundant in the central region of the body. In the pedal groove area, the sclerites have a characteristic arrangement (Fig. 2c1, c2). There are a few leaf-shaped scales (50-60 µm long, 20 µm wide) (Fig. 2c4) inserted between long hollow flat knife-shaped sclerites (150–200 µm long, 15-20 μm wide) (Fig. 2c1, c2) and hollow knife-shaped sclerites with a keel (100–180 µm long, 15–20 µm wide) (Fig. 2c3).

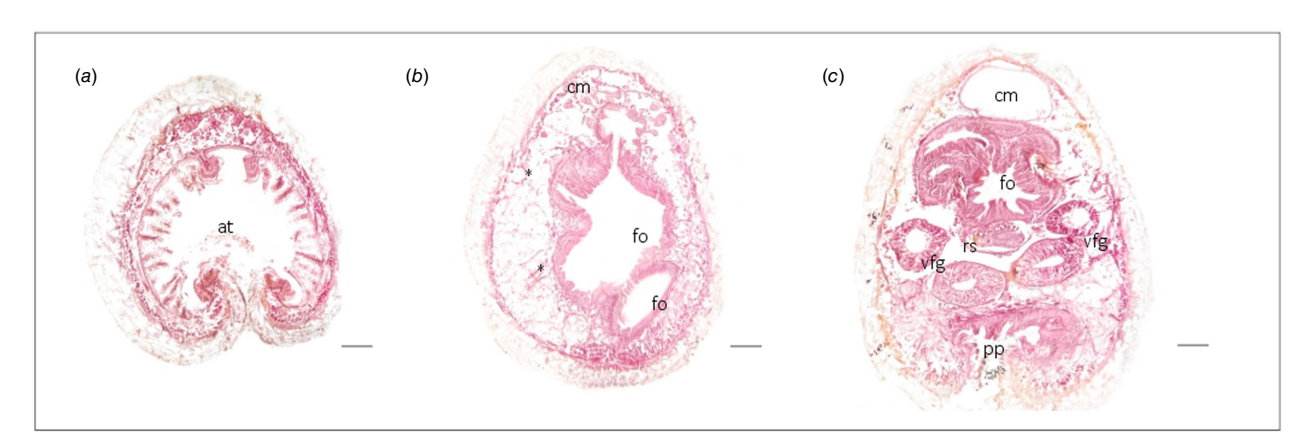


Fig. 6. Serial sections of the anterior region of the holotype of *Proneomenia occulta* sp. nov. Sections (*a–c*) correspond with areas in the reconstruction in Fig. 4c. Abbreviations as per Fig. 4. Scale bars: 100 μm.

## Pedal groove and pallial cavity

Ciliated and glandular pedal pit ( $340\,\mu m$  long,  $80\text{-}400\,\mu m$  wide,  $90\text{-}110\,\mu m$  high). The anterior follicular pedal glands end latero-dorsally in the pedal pit and continue ventrally as a single package to the foregut (Fig. 4c, section c). The pedal pit gives rise to a single triangular pedal fold that retains the shape and size ( $15\text{-}20\,\mu m$  wide,  $60\text{-}65\,\mu m$  high) throughout the body. The pallial cavity opens ventrally. The posterior sections were overstained, thereby making an accurate reconstruction and complete measurements of many structures impossible. Nevertheless, all structures could be identified. The rectum opens dorsally and the spawning ducts (fused to a single tube) open ventrally in the cavity, not creating a sphincter. Without respiratory folds.

# Digestive system

The mouth opens at the posterior end of the atrium and continues as a wide foregut (380-400 µm wide, 400-450 µm high) (Fig. 4c). The foregut (710 µm long) is folded in the anterior region, with a ventral and a dorsal bag or pocket (Fig. 4c, section b; Fig. 6b, c). Towards the radular region and in this area, the pharynx becomes narrower (500 µm wide,  $90-100 \,\mu m$  high) (Fig. 4c, section c; Fig. 6c). The radula is polystichous with a single posterior radular sac (200 μm long, 250–280 μm wide, 200 μm high) (Fig. 6c) and 12 single equal teeth per row. The teeth have a small base (7.5 µm wide) and are straight. The ventrolateral foregut glands are of type-C-Epimenia-type, the tubes that open into the foregut anteriorly to the radular sac are formed by two coiled, long tubes (Fig. 4c, 6c). The midgut has a small, short dorsal caecum (480 µm long, 200–320 µm wide, 150-200 μm high) (Fig. 4c, 6b, c). Without clear lateral constrictions of the midgut.

## Cerebral ganglion and sense organs

The cerebral ganglion (190 µm long, 200 µm wide, 50–100 µm high) is elliptical in cross-section and located dorsally to the mouth and anterior part of the foregut (Fig. 4c). The atrium has a small anterior cavity (110 µm long, 100 µm wide, 80–100 µm high). The opening of the atrium gives way to a large cavity (480 µm long, 320–500 µm wide, 200–500 µm high). The atrium has ~24 simple papillae (20 µm wide, 80 µm high) and four large papillae, two dorsal (90 µm wide, 70 µm high) and two ventral (105 µm wide, 100 µm high), on both sides of the opening (Fig. 4c, section a; Fig. 6a) that form the atrial sense organ. Dorsoterminal sensory organ not observed; although there are signs of a possible organ, the sections in this region are too damaged to determine this with certainty.

#### Gonopericardial system

Making an accurate reconstruction of the structures was not possible due to overstaining of the posterior sections but most of the organs were identified and followed in the sections. There were no copulatory stylets or abdominal spicules. The spawning ducts were paired at the origin where these connected with the pericardioducts. The spawning ducts fused into a single duct in this organ's mid-region. Determining whether the pericardium is paired in the posterior region was not possible. Remains of a single pair of seminal receptacles were observed.

#### Remarks

Although the quality of the serial sections did not allow us to conduct a complete reconstruction of the posterior organs, we could identify and characterise the most critical characters to place this species into a genus and provide distinction from other described species. For example, we could determine that this species does not have copulatory stylets and therefore classify this as a species of Proneomenia. This was important because in the first sorting of the collection into morphospecies, this specimen was considered to be of the same species as the *Dorymenia* species described below; the two specimens were found in the same locality and are similar in external appearance, although the digitiform projection of Proneomenia occulta sp. nov. is not evident in the Dorymenia described here. The phylogenetic analysis of DNA barcodes and the species delimitation analysis also clearly show that the specimens belong to species of the two different genera of Proneomeniidae (see below).

Considering the external aspect and important internal characteristics (Tables 3, 4), the specimen examined here does not belong to any described species of Proneomenia and constitutes a species new to science. The lack of protuberances or a keel makes P. occulta sp. nov. different from P. custodiens, P. epibionta and P. stillerythrocytica (Salvini-Plawen 1978; Todt and Kocot 2014), all with a dorsal keel and from P. praedatoria that has seven protuberances (Salvini-Plawen 1978) (Table 3). The new species (17.5  $\times$  2.5 mm) is smaller than P. sluiteri (up to  $150 \times 12 \,\mathrm{mm}$ ) (Hubrecht 1880), P. gerlachei and P. bulbosa (both  $\sim$ 45  $\times$  2.5 mm) (Pelseneer 1901; García-Álvarez et al. 2009), and P. valdiviae and P. hawaiiensis (36-37  $\times$  2 mm) (Thiele 1903; Heath 1905) (Tables 3, 4). There are no data on the length of P. insularis as this was described based on an anterior fragment (Heath 1911) but the new species has 12-14 teeth per row whereas P. insularis has 24 teeth per row (Table 4). The size of the new species is comparable to that of P. acuminata  $(20-30 \times 1.8 \,\mathrm{mm})$  but this has fewer teeth per row (P. acuminata has 28) and lacks seminal vesicles whereas P. acuminata has one (Wirén 1892; García-Álvarez et al. 2009). P. occulta sp. nov. most closely resembles P. desiderata of all the species in the genus, considering the external anatomical characters (digitiform projection and lack of keels or protuberances) and the number of radular teeth per row (14) (Tables 3, 4). However, the new species lacks abdominal spicules that are present in P. desiderata (Kowalevsky and Marion 1887).

# Proneomenia satiata Cobo & Kocot, sp. nov.

(Fig. 1b, 2b, 3b, 4d, e, 7.)

ZooBank: urn:lsid:zoobank.org:act:264F2A13-B5E1-451F-9126-910619 D4CBB2

# Type material

**Holotype.** MNHN-IM-2013-61611 serial sections of the anterior and posterior region (58 slides; anterior region 8  $\mu$ m, posterior region 5  $\mu$ m), fragment of the central region preserved in 96% ethanol, light microscopy preparations of the sclerites (4 slides), SEM preparations of sclerites (1 stub), DNA barcodes (GenBank: OQ600026; OQ597880); South China Sea, ZhongSha 2015 expedition station CP4133, 999–1071-m

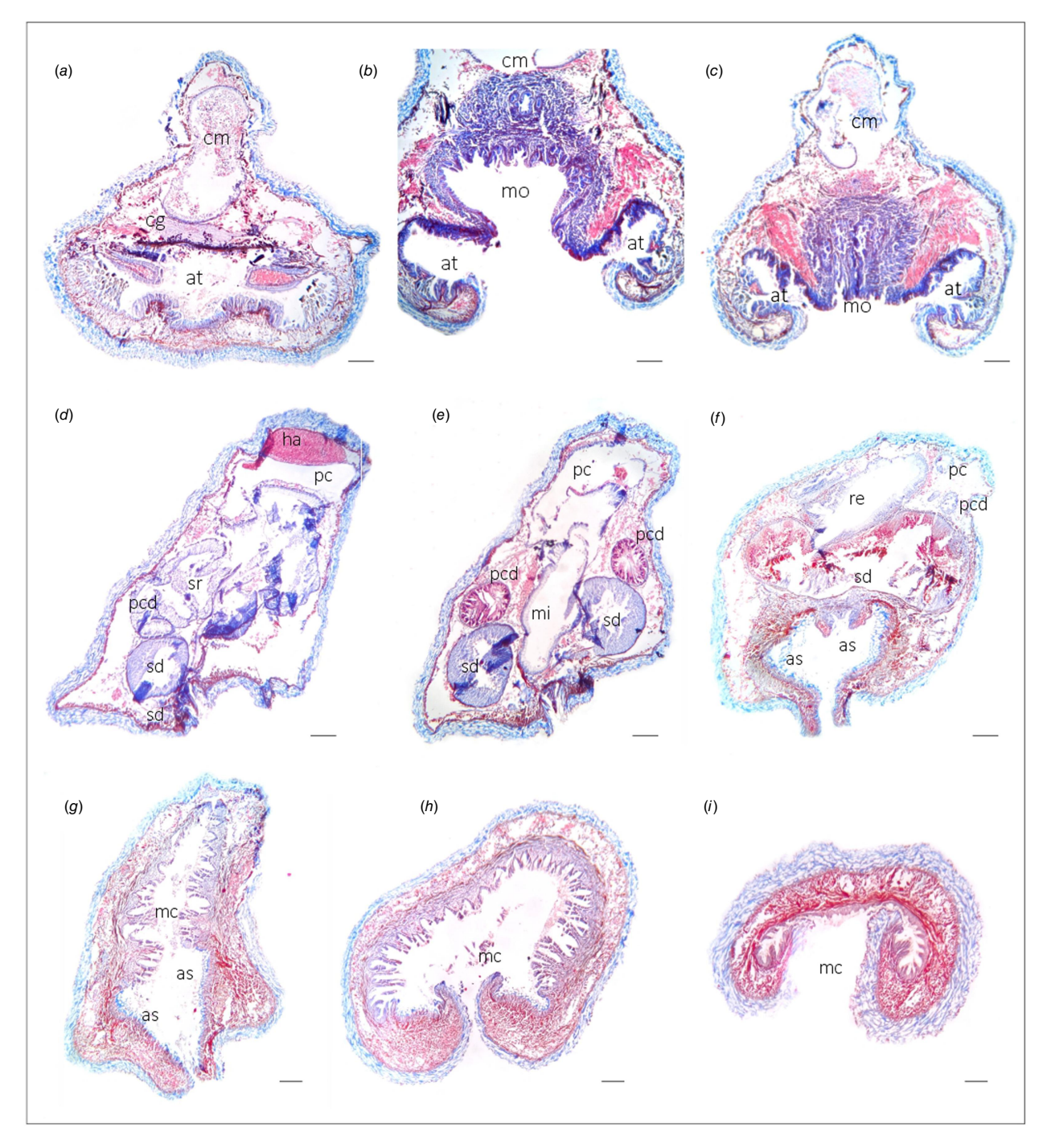


Fig. 7. Serial sections of the holotype of *Proneomenia satiata* sp. nov. Anterior (a-c) and posterior region (d-i). Abbreviations as per Fig. 4. Scale bars: 200  $\mu$ m.

depth. Type series deposited at the Muséum National d'Histoire Naturelle, Paris (MNHN).

# **Diagnosis**

Large, elongate animal (holotype 110 mm long and 1.8–4.8 mm wide). Rounded anterior end and posterior end with a marked digital projection. Light cream to white-coloured in 96% ethanol. The sclerite cover is very dense and therefore the animal does not appear scaly. Slight dorsal keel. Pedal groove, pedal pit and pallial cavity externally evident. Thick cuticle with straight hollow acicular sclerites of seven different distinguishable morphotypes. Polystichous radula with 21–22 uniform teeth per row. Numerous small, single atrial papillae. Without copulatory stylets. With numerous abdominal spicules (bundles of least 75 spicules, arranged in three layers). With four globular seminal receptacles attached to each pericardioduct. With a dorsoterminal sensory organ not evident externally. Pallial cavity with folded epithelium.

# Distribution and ecology

South China Sea (Pacific Ocean) (ZhongSha 2015; station CP4133; 19°59′N–116°24′E; 999–1071-m depth). Feeding on Octocorallia.

# **Etymology**

From Latin satiatus, satiata satiatum, meaning satiated. In allusion to the fact that the specimen was feeding and with the mouth full of food when captured.

## **Description**

# **Habitus**

Large elongate animal (110 mm long and  $1.8-4.8 \, \text{mm}$  wide) (Fig. 1b). The anterior body region has a rounded end (Fig. 1b2) and the posterior end, that is nearly straight, has a clear finger-like projection (Fig. 1b2). Pedal groove, mouth and opening of the pallial cavity marked externally. Light cream to white in 96% ethanol (Fig. 1b). Specimen stiff due to thick cuticle and skeletal sclerites, although not perfectly preserved; folded and broken near the midposterior region. There is no evident dorsal keel externally, although the folding of the body, due to preservation, could obscure this: the serial sections show a slight keel, especially in the anterior region (Fig. 7a, c).

#### **Mantle**

Thick cuticle (90–125  $\mu$ m) with epidermal papillae and hollow acicular sclerites inserted in several layers (Fig. 2b3). Although all the sclerites are very similar in shape at first glance, six types of hollow acicular sclerites are distinguishable. (1) The most abundant type consists of hollow, slightly curved sclerites with a truncated proximal end (region inserted in the cuticle = base of the sclerite), a pointed distal end and internal cavity that can extend towards the central or the distal

end of the sclerite (420-510 µm long, 20-30 µm wide) (Fig. 2b3, 3b1, b2, b4). Some of these can be much smaller (150-210 µm long, 20 µm wide) (Fig. 2b3, 3b4) than most of the sclerites. (2) Hollow slightly curved acicular sclerites with a curvature in the proximal rounded end and an internal cavity that does not reach the central region of the sclerite  $(220-400 \,\mu\text{m} \, \log, \, 20-30 \,\mu\text{m} \, \text{wide}) \, (\text{Fig. } 3b1). \, (3) \, \text{Hollow}$ straight acicular sclerites with a truncated proximal end and with the internal cavity along the entire length of the sclerite (150–220 µm long, 20–30 µm wide) (Fig. 3b1, b3). (4) Hollow short acicular sclerites with a small internal cavity restricted to the base of the sclerite (150-300 µm long, 15-20 µm wide) (Fig. 3b3). (5) Small, thin curved hollow acicular sclerites (50–100 μm long, 5–8 μm wide) (Fig. 3b4); (6) Long, straight, thin acicular sclerites with the internal cavity that extends towards the distal end of the sclerite, most of these sclerites are broken in the preparations (400-580 μm long, 5-15 μm wide) (Fig. 3b5). All these sclerites were found along the entire body, although the long straight sclerites (Fig. 3b5) are more abundant in the ventral region. A more detailed study, to determine if there is a regional distribution of the sclerites as described for other species (Scheltema and Ivanov 2000; Todt and Kocot 2014), would be desirable if more specimens were available. Special scales or arrangement of the sclerites along the pedal groove were not observed (Fig. 2b1).

#### Pedal groove and pallial cavity

The pedal pit is small in relation to the size of the animal  $(485 \,\mu\text{m long}, 100-115 \,\mu\text{m wide}, 45-50 \,\mu\text{m high})$  (Fig. 4d). This opens in the radular region and gives rise to a single pedal fold (80-90 µm high, 70-80 µm wide). In the posterior part of the body two additional folds, similar in shape and size (80 µm high, 70 µm wide), flank the original pedal fold (Fig. 7f). These enter in the pallial cavity. The pallial cavity is large  $(4500 \, \mu m \, long, \, 225-1250 \, \mu m \, wide, \, 225-1250 \, \mu m$ high) and opens ventrally (Fig. 4e). The epithelium of the cavity is ciliated and folded. The folds are equidistantly distributed in the cavity (Fig. 7f-i). Some of these are branched but many appear broken in the sections. The interpretation of the function of these folds is under question. Although the histology does not closely resemble the respiratory folds of other solenogasters and these organs were not described in other Proneomenia species, the function as respiratory folds cannot be completely discarded. The pallial cavity of this species is considerably large and the folds are present throughout this. The cavity continues to the most posterior region of the body (in the finger-like projection) as a straight tube (225 µm long, 100-200 µm in diameter) (Fig. 4e). The rectum opens dorsally and the spawning ducts (fused into a wide single tube) open ventrally in the cavity (Fig. 4e).

#### Digestive system

The animal was feeding at the time of fixation. Remains of an octocoral polyp (not identified) were found protruding from the mouth. This made reconstruction of the digestive

tract significantly more difficult, nevertheless all organs could be identified and reconstructed.

The mouth opens at the posterior end of the atrium (mouth opening 672 µm long) (Fig. 4d), surrounded by a strong layer of musculature (200–350 µm thick) (Fig. 7b, c). The opening was preceded by a heavily glandular region  $(100 \, \mu m \, long, \, 2125 \, \mu m \, wide, \, 875-500 \, \mu m \, high; \, Fig. \, 7b, \, c)$ . The mouth continues dorsally as a straight tube (400 µm long, 225 µm wide, 150 µm high) (Fig. 4d). As the animal was feeding at the time of fixation, the mouth and anterior region of the foregut were assumed to be extended, hence the pharynx appears large in the most anterior region and continues as a large glandular tube (1650 µm long, 600-750 µm wide, 1500-2000 µm high) until this merges with the midgut. In the anterior region, the foregut has two anterior bags, one dorsal to the mouth opening (250 µm long, 625 µm wide, 150 µm high) and a ventral one that is larger and posterior to the mouth opening (375 µm long, 625-750 µm wide, 150 µm high (Fig. 4d). The midgut caecum is situated far anteriorly preceding the atrium (Fig. 4d, section a; Fig. 7a), increasing in size from the anterior region of the body until fusing with the foregut dorsally  $(4200 \,\mu\text{m} \, long, \, 400-1075 \,\mu\text{m} \, wide, \, 370-2075 \,\mu\text{m} \, high).$ Numerous cnidocytes were visible in the anterior region of the dorsal caecum.

The radula is polystichous with 21–22 uniform teeth with a small base, and with a small posterior double radular sac (160  $\mu$ m long, 350  $\mu$ m wide, 200  $\mu$ m high) (Fig. 4*d*). The ventrolateral foregut glands of the type-C–*Epimenia*-type open into the pharynx at both sides of the radular sac (Fig. 4*d*, section c; Fig. 7*c*), continuin as two long, coiled tubes, with some of the turns directed far toward the anterior region of the pharynx. The midgut has slightly marked lateral constrictions. The rectum, that is long (750  $\mu$ m long) and profusely ciliated, terminates mid-dorsally in the anterior pallial cavity (Fig. 4*e*).

## Cerebral ganglion and sense organs

The cerebral ganglion (312 µm long, 475 µm wide, 96-168 µm high) is oval in cross-section and located far anteriorly, dorsal to the central part of the atrium and anterior to the atrial opening to the exterior (Fig. 4d, section a; Fig. 7a). The atrium (2625 μm long, 525-2175 μm wide, 150-625 µm high) opens ventrally to the exterior (opening 600 µm long) (Fig. 4d). Anteriorly to the opening, the atrium has a prolongation (2025 µm long, 150-500 µm high, 525–1525 µm width; Fig. 4d, section a; Fig. 7a), where most of the numerous small single papillae are located and continues posteriorly as two small cavities (475 µm long, 650 µm wide, 375 µm high) at both sides of the mouth opening (Fig. 7b, c). In addition to the single papillae, there are two dorsal and two large ventral papillae (3-8 × 2-4 µm) surrounding the opening of the atrium (Fig. 7a, b). With a small (405 µm long, 200-250 µm in diameter) dorsoterminal sensory organ, located dorsally to the opening of the pallial cavity, anterior to the finger-like projection. The dorsoterminal sensory organ is not evident externally.

# Gonopericardial system

The pericardium (3050 μm long reconstructed, 300-500 μm in diameter) becomes smaller in the more posterior region where paired (50-75 µm in diameter) (Fig. 7f). The heart (750 µm long) is attached dorsally in the anterior region (Fig. 4e, 7d). The pericardioducts (3125  $\mu$ m long; 25–100  $\mu$ m in diameter) connect to the pericardium in the paired region. These join the spawning ducts in the posterior region, where a cluster of four globular seminal receptacles is connected to each pericardioduct (Fig. 7d). The spawning ducts are paired at the origins and along most of the length (3250 µm long, 300–550 μm wide, 125–850 μm high) (Fig. 7d, e). These fuse (Fig. 7f) and open laterally into the pallial cavity as a single duct (1125 μm long, 1000–1100 μm wide, 100–500 μm high) (Fig. 4e). Without copulatory spicules. With two large bundles of abdominal spicules (1780 µm long, with at least 75 spicules arranged in three layers of 50-70 µm with) at both sides of the opening of the pallial cavity (Fig. 7f, g).

## **Remarks**

The lack of copulatory stylets justifies the inclusion of this species in the genus Proneomenia. P. satiata sp. nov. has a slight dorsal keel, a character shared with P. custodiens, P. epibionta and P. stillerythrocytica (Salvini-Plawen 1978; Todt and Kocot 2014) and distinguishes this species from P. praedatoria that has seven protuberances (Salvini-Plawen 1978), and from the rest of the species of the genus that all lack these features (Tables 3, 4). The new species has a marked posterior finger-like projection, a character present in many species of Proneomenia but the known species with a slight dorsal keel all have rounded posterior ends without such a projection (Salvini-Plawen 1978; Todt and Kocot 2014). In addition to these external differences, P. satiata has fewer radular denticles (~21) than P. epibionta and P. stillerythrocytica (with 41-56) (Salvini-Plawen 1978; Todt and Kocot 2014) (Table 3). The number of teeth and seminal receptacles of P. satiata sp. nov. and P custodiens are comparable (three receptacles described for P. custodiens), nevertheless the new species lacks the brooding chamber characteristic of the Icelandic P. custodiens (Todt and Kocot 2014) and the external aspect of both species is clearly different. In addition to being the only species with four seminal receptacles connected to each pericardioduct, this species differs from the remaining species of the genus in the number of teeth of the radula (Tables 3, 4). In addition, P. satiata sp. nov. is significantly larger (especially in length;  $110 \times 3-5 \,\mathrm{mm}$ ) than all known species of the genus except P. sluiteri that is similar in length but wider (105–150 × 11–12 mm) (Hubrecht 1880; Heath 1918; Kocot and Todt 2014). Nevertheless, there are differences in the internal anatomy between these two species (Tables 3, 4). The external aspect is useful to differentiate

*P. satiata* sp. nov. from the previously described *Proneomenia* species. This, combined with the differences in some important internal characters, justifies the designation as a new species. Besides, the DNA barcode sequences obtained and species delimitation analyses confirm the differentiation between the three new species of *Proneomenia* described here (see below).

# Genus Dorymenia Heath, 1911

Type species: Dorymenia acuta Heath, 1911.

# **Species included**

D. acutidentata Salvini-Plawen, 1978; D. antarctica (Thiele, 1913): D. cristata Salvini-Plawen, 1978; D. discovervi (Nierstrasz, 1908); D. harpagata Salvini-Plawen, 1978; D. hesperidesi García-Álvarez, Urgorri & Salvini-Plawen, 2000; D. hoffmani Salvini-Plawen, 1978; D. interposita Salvini-Plawen, 1978; D. longa (Nierstrasz, 1902); D. menchuescribanae García-Álvarez, Urgorri & Salvini-Plawen, 2000; D. parvidentata García-Álvarez & Urgorri, 2003; D. paucidentata Salvini-Plawen, 1978; D. peroneopsis Heath, 1918; D. profunda Salvini-Plawen, 1978; D. quincarinata (Ponder, 1970); D. sarsii (Koren & Danielssen, 1877); D. singulatidentata Salvini-Plawen, 1978; D. tetradoryata Salvini-Plawen, 1978; D. tricarinata (Thiele, 1913); D. troncosoi García-Álvarez, Urgorri & Salvini-Plawen, 1998; D. usarpi Salvini-Plawen, 1978; D. vagans (Kowalevsky & Marion, 1887); D. weberi (Nierstrasz, 1902); D. ancora McCutcheon, Kocot & Cobo, 2022; D. tanifa McCutcheon, Kocot & Cobo, 2022; D. lucida McCutcheon, Kocot & Cobo, 2022.

## Diagnosis (amended)

Thick cuticle with epidermal papillae. Hollow acicular sclerites arranged in several layers. Polystichous radula. Foregut glands of type-C–*Epimenia*-type. Midgut with constrictions. Usually with at least one pair of seminal receptacles. Secondary genital opening unpaired. With copulatory stylets. With dorsoterminal sense organ(s). Without respiratory folds.

# Dorymenia boucheti Cobo & Kocot, sp. nov.

(Fig. 1d, 2d, 3d, 8, 9.)

ZooBank: urn:lsid:zoobank.org:act:071657FB-0257-4DD0-AA26-A7C534 B9B5C1

## Type material

**Holotype.** MNHN-IM-2013-50092 in serial sections of the anterior and posterior region (20 slides,  $5 \mu m$ ), fragment of the central region preserved in 96% ethanol, light microscopy preparations of the sclerites

(3 slides), SEM preparations of sclerites (2 stubs), DNA barcodes (GenBank: OQ600025; OQ597881); South China Sea, DongSha expedition (2014) station CP4123, 1612–1666-m depth. Type series deposited at the Muséum National d'Histoire Naturelle, Paris (MNHN).

## **Diagnosis**

Robust animal (12.5 mm long and 1.5 mm wide) with a truncated anterior end and rounded, straight posterior end. Ochre in 96% ethanol. Sclerites and pedal groove evident externally. Thick cuticle with straight and curved hollow acicular sclerites. With scales of the pedal groove. Radula with 20 elongate teeth per row. With a pair of single copulatory stylets. Without abdominal spicules. Without seminal receptacles. With a dorsoterminal sensory organ.

#### Distribution

South China Sea (Pacific Ocean) (DongSha 2014; station CP4123, 21°36′N, 118°16′E; 1612–1666-m depth).

# **Etymology**

Male genitive in honour of Dr Philippe Bouchet, an outstanding scientist and colleague, who kindly provided the material from the South China Sea and for his supportive role in the first author's career.

## **Description**

#### **Habitus**

Robust animal (12.5 mm long and 0.5-1.5 mm wide) with the arrangement of the sclerites evident externally. The anterior region, with a blunt end, is wider than the posterior that has a rounded end. Pedal groove marked externally. Ochre in 96% ethanol (Fig. 1d).

#### **Mantle**

Thick cuticle, slightly thinner in the ventral region (70–200 µm). With epidermal papillae. With hollow acicular sclerites, pallet-shaped sclerites and scales along the pedal groove. The small pallet-shaped sclerites appear mostly on the dorsal region of the body (80-100 µm long, 5-8 µm wide) (Fig. 2d3, 3d1, d2). There are three types of hollow acicular sclerites: (1) slightly curved hollow acicular sclerites with a rounded distal end and internal cavity towards most of the sclerite (140–200 µm long, 10–15 µm wide) (Fig. 2d2, d4, 3d3); (2) straight hollow acicular sclerite with the internal cavity along the entire length of the sclerite  $(140-200 \,\mu\text{m} \, long, \, 10-15 \,\mu\text{m} \, wide)$  (Fig. 3d4); (3) straight hollow acicular sclerites with a curvature at the proximal end and the internal cavity along the entire length of the sclerite (140–200 µm long, 10–15 µm wide) (Fig. 3d4). The special scales along the pedal groove are long, flat knife-shaped scales (200 µm long, 15–20 µm wide) (Fig. 2d1).

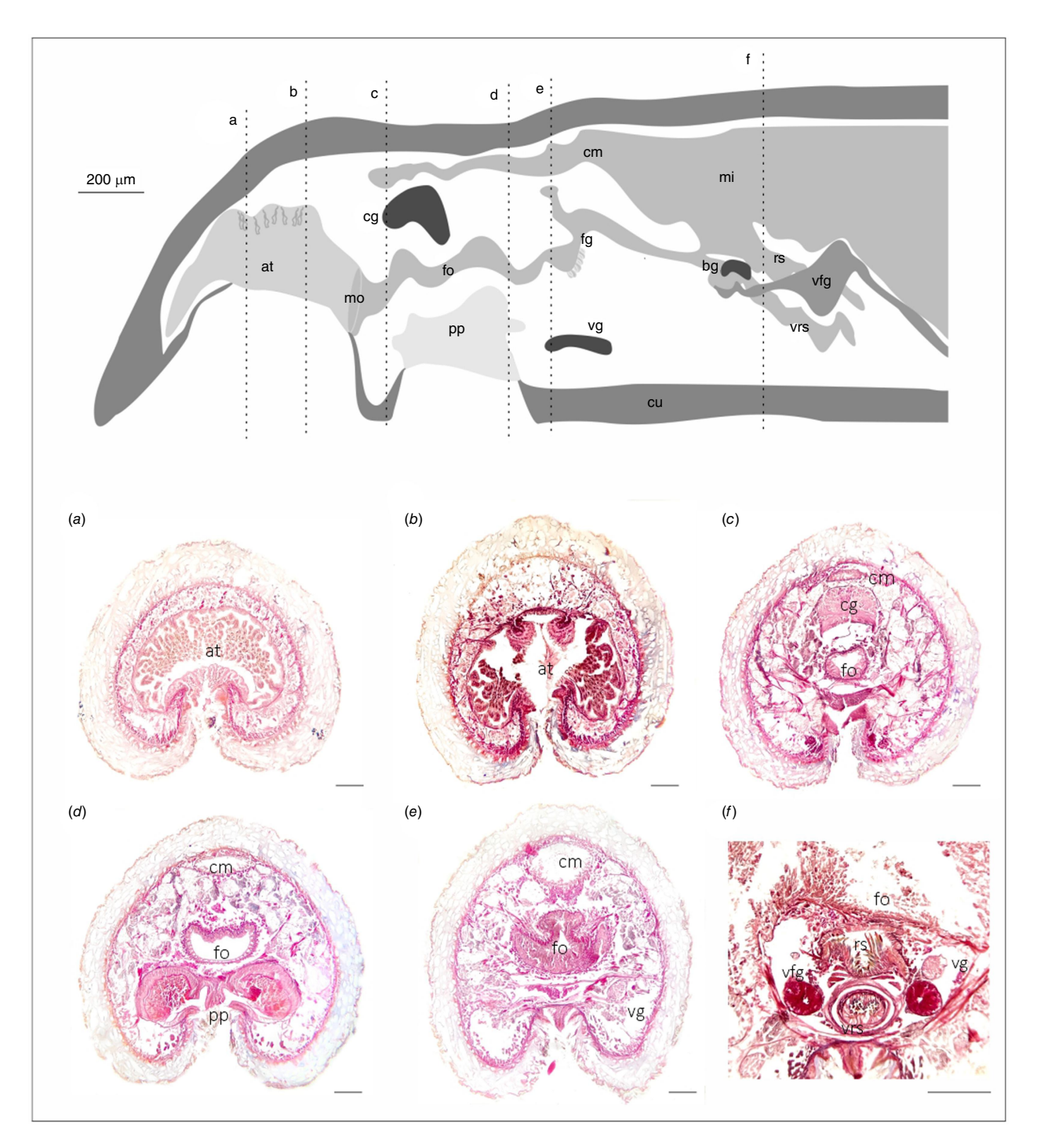


Fig. 8. Reconstruction of the internal anatomy of the anterior region of *Dorymenia boucheti* sp. nov. and serial sections of the holotype (a-f) correspond with the lines in the reconstrusction. Abbreviations as per Fig. 4. Scale bars:  $100 \, \mu m$ .

# Pedal groove and pallial cavity

The pedal pit (350  $\mu$ m long, 130–340  $\mu$ m wide, 30–130  $\mu$ m high) is strongly ciliated, especially in the posterior region that is also highly glandular and forms two internal extensions (70  $\mu$ m long) (Fig. 8*d*). The pedal pit has three folds with the central fold larger than the lateral ones (20–25  $\mu$ m wide, 50  $\mu$ m high). The anterior follicular pedal glands form a

large glandular package that surrounds the foregut at the anterior region and opens dorsally into the pedal pit. The pallial cavity opens ventrally; is small and the walls are slightly folded (Fig. 9). The pallial cavity has a posterior prolongation (80  $\mu$ m long, 90–120  $\mu$ m in diameter) (Fig. 9). The rectum opens dorsally and the spawning ducts (fused to a single tube) open in the centre of the cavity (Fig. 9b).

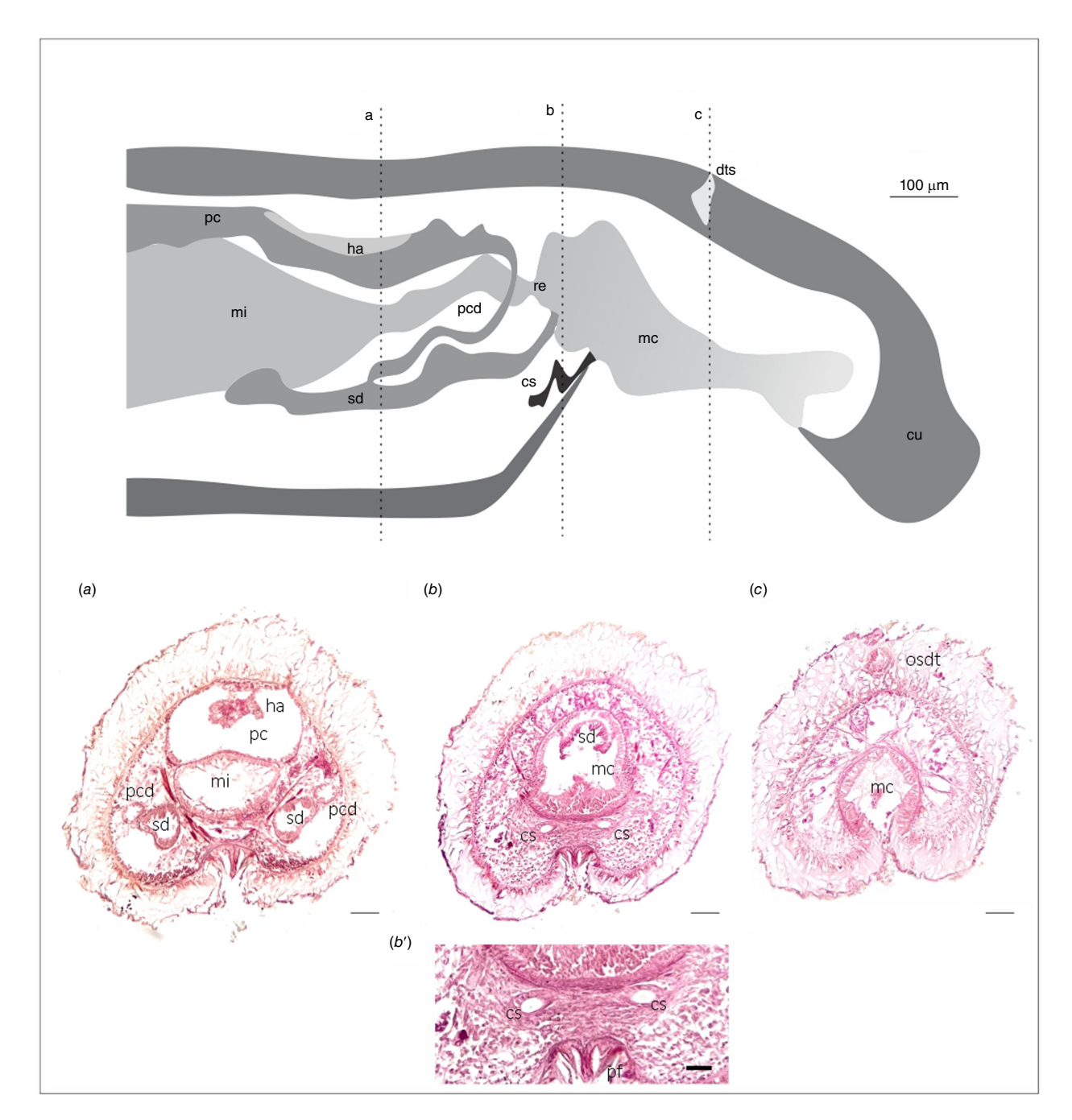


Fig. 9. Reconstruction of the posterior internal anatomy of *Dorymenia boucheti* sp. nov. and serial sections of the holotype (a-c) correspond with the lines in the reconstruction. Abbreviations as per Fig. 4. Scale bars: a-c, 100  $\mu$ m; b', 10  $\mu$ m.

# Digestive system

The mouth opens at the posterior end of the atrium and continues as a rounded, tubular foregut that runs almost parallel to the pedal groove (1300  $\mu$ m long, 100–120  $\mu$ m in diameter) (Fig. 8c). In the central region, the rounded foregut is U-shaped (200–210  $\mu$ m wide, 80–100  $\mu$ m high) (Fig. 8d) and has an elongated dorsal pocket without glandular function (Fig. 8e). In this region, a package of glands discharges in the ventral wall of the foregut. The radula is

polystichous with a radular sac that is paired posteriorly (320  $\mu$ m long, 100–120  $\mu$ m wide, 50–80  $\mu$ m high) (Fig. 8e, f) and with a ventral radular sac (= subradular pouch) of the same dimensions. There are 20 teeth per row. The teeth have a small base (4.5  $\mu$ m wide) and are elongated (7–9.4  $\mu$ m long, 1.5–3  $\mu$ m wide) (Fig. 8f). The ventrolateral foregut glands are of type-C–*Epimenia*-type and the tubes are long and straight, without loops (Fig. 8e, f). With a long, straight dorsal caecum (1040  $\mu$ m long, 40–100  $\mu$ m wide,

 $30\text{--}100\,\mu m$  high). The midgut is without serial constrictions. The rectum is triangular in cross-section.

# Cerebral ganglion and sense organs

The cerebral ganglion (180  $\mu$ m long, 100–200  $\mu$ m wide, 80–180  $\mu$ m high) is almost circular in cross-section (Fig. 8c), becoming paired in the posterior region. The atrium is a rounded cavity (360  $\mu$ m long, 250–500  $\mu$ m wide, 80–250  $\mu$ m high) that opens ventrally (Fig. 8a). There are numerous single papillae (Fig. 8a) and four larger ones (80–100  $\mu$ m wide): two attached to the dorsal wall and a ventral pair with one on either side of the atrial opening, interpreted as the atrial sense organ. With a rounded dorsoterminal sensory organ (35  $\mu$ m long, 35–40  $\mu$ m in diameter) located dorsally to the central region of the pallial cavity (Fig. 9c).

## Gonopericardial system

The pericardium (340 μm long reconstructed, 40–200 μm in diameter) has a straight, paired posterior region where the pericardioducts are attached (Fig. 9). The two heart chambers are easily distinguished. The heart is attached to the dorsal wall of the pericardium in the midregion. The pericardioducts (220 µm long, 10-40 µm in diameter) connect to the spawning duct in the midregion (Fig. 9a). The spawning ducts are paired at the origins (220 µm long, 10-40 µm in diameter) (Fig. 9a) and fused as a single tube in the mid-posterior region (300 µm long, 40–100 µm wide,  $20-80 \,\mu m$  high). This single duct (130  $\mu m$  long, 80–100  $\mu m$ wide, 20-40 µm high) opens centrally in the anterior region of the pallial cavity (Fig. 9). The opening is straight but without a clear sphincter. With a pair of single rounded copulatory spicules (120 µm long internally; 8–10 µm in diameter) (Fig. 9b, b'). Seminal receptacles were not observed.

#### Remarks

Dorymenia is the only genus of the two included in Proneomeniidae with copulatory stylets (Scheltema and Schander 2000; García-Álvarez and Salvini-Plawen 2007; García-Álvarez et al. 2009). Therefore MNHN-IM-2013-50092 was identified as a Dorymenia species. Considering the geographical distribution and in view of the combination of internal characters and habitus, D. boucheti sp. nov. differs enough from the remaining described species of the genus to determine that this constitutes a new species. Within Dorymenia, there are currently 28 described species with a worldwide distribution (Koren and Danielssen 1877; Kowalevsky and Marion 1887; Nierstrasz 1902; Heath 1911, 1918; Ponder 1970; García-Álvarez et al. 2000; García-Álvarez and Urgorri 2003; García-Álvarez and Salvini-Plawen 2007; García-Álvarez et al. 2009; Pedrouzo et al. 2014; McCutcheon et al. 2022). The importance of the radula to the differentiation and grouping of Dorymenia species was pointed out by several authors (Salvini-Plawen 1978; García-Álvarez et al. 2000; Scheltema and Schander 2000; García-Álvarez and

Urgorri 2003). This was consequently emphasised in the latest description of species of this genus (McCutcheon *et al.* 2022) that includes a simplification of the nomenclature used for the radula types within *Dorymenia* (following García-Álvarez *et al.* 2000; García-Álvarez and Urgorri 2003): (a) radula with uniform teeth (that can have long or short bases), with a curved apical tip; (b) radula with elongated teeth; or (c) radula with one or two medial teeth.

The radula in D. boucheti sp. nov. has elongated teeth. Four of the known species of the genus, D. acutidentata, D. singulatidentata, D. paucidentata, D. parvidentata and D. quincarinata have the same type of radula (Salvini-Plawen 1978; García-Álvarez et al. 2000; García-Álvarez and Urgorri 2003; McCutcheon et al. 2022). Externally, D. boucheti sp. nov. lacks keels or body protuberances what make it different from D. quincarinata that has five longitudinal ridges (Ponder 1970; Salvini-Plawen 1978; McCutcheon et al. 2022). D. boucheti sp. nov. is relatively smaller  $(12.5 \times 1 \text{ mm long})$  than D. acutidentata  $(22 \times 1.5 \text{ mm})$ and D. singulatidentata (30  $\times$  2 mm). D. boucheti sp. nov. is similar in size to D. paucidentata but these species differ in the number of teeth per row (20 in the new species 14 in D. paucidentata) and, whereas D. boucheti sp. nov. has a paired posterior pericardium, this organ is consistently unpaired in D. paucidentata (Salvini-Plawen 1978). In addition, the copulatory stylets are rounded in the new species but have a quadrangular cross-section at the distal end in D. paucidentata (Salvini-Plawen 1978). Finally, D. boucheti sp. nov. can be distinguished from D. parvidentata in that this species is larger than D. parvidentata, reaching 7 mm long (García-Álvarez and Urgorri 2003), there is an atriobuccal cavity whereas D. parvidentata has two different openings to the exterior, the copulatory stylets are rounded, whereas in D. parvidentata these are starshaped in cross-section and the new species has 20 teeth per row whereas D. parvidentata has 10-12 teeth per row (García-Álvarez and Urgorri 2003).

There is no information available on the shape and arrangement of the teeth in two *Dorymenia* species, *D. peroneopsis* and *D. tetradoryata* and therefore these cannot be classified as having one of the aforementioned types of radula (McCutcheon *et al.* 2022). Nevertheless, there is information about the number of teeth for *D. tetradoryata* that has nine (Salvini-Plawen 1978), significantly fewer than in *D. boucheti* sp. nov. and the new species can be distinguished externally from *D. peroneopsis* as the latter has a marked posterior finger-like projection (Heath 1918).

The absence of seminal receptacles in *D. boucheti* sp. nov. should be noted. Seminal receptacles are present in almost all species of the genus, although there are other exceptions such as *D. quincarinata* and information is not available for some species (McCutcheon *et al.* 2022). Therefore, we have amended the diagnosis of the genus to include the possible absence of this character.

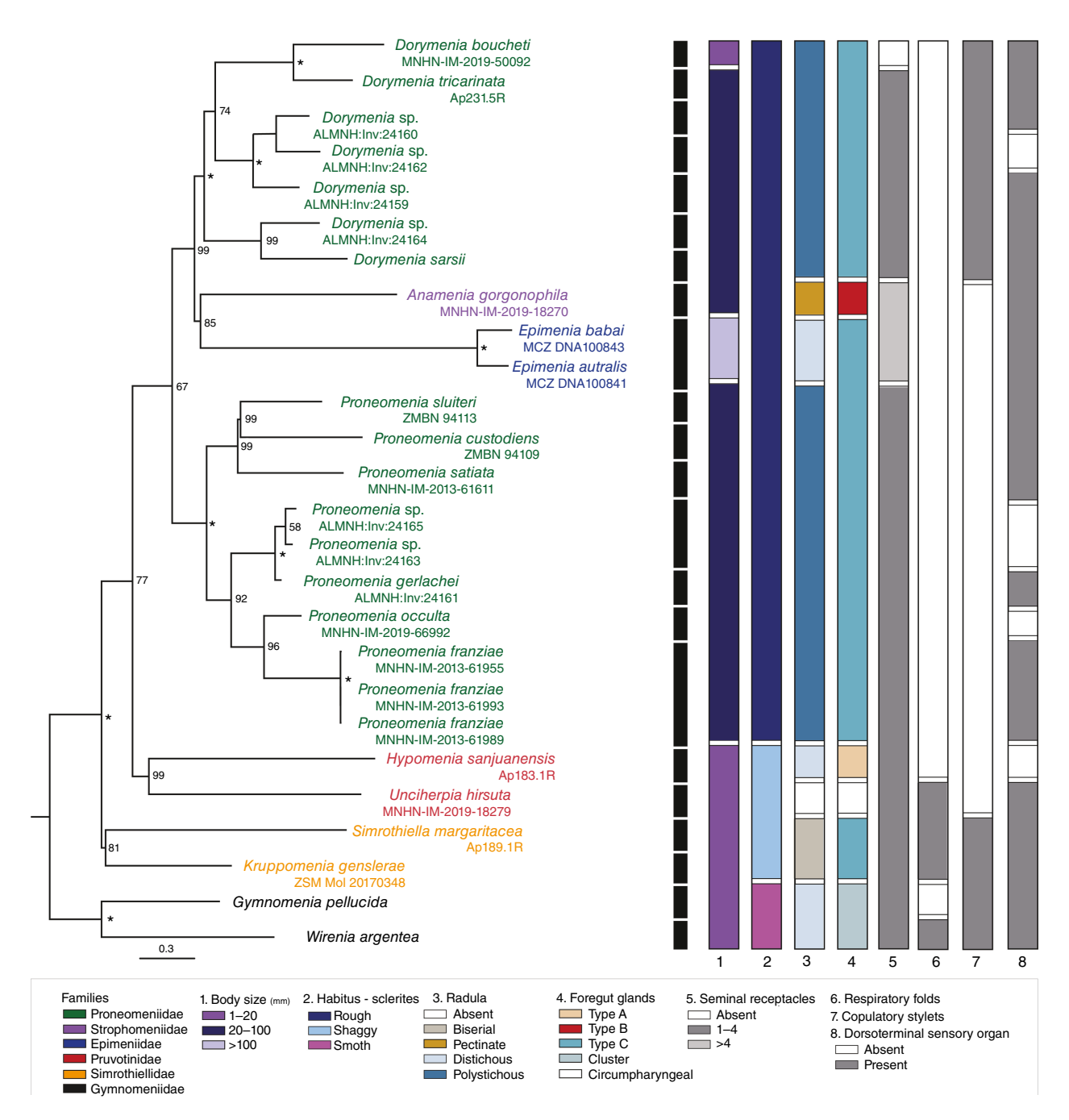


Fig. 10. Maximum likelihood phylogenetic reconstruction based on 16S and COI genes showing the relationship between Proneomenia and Dorymenia. Bootstrap support values are shown at each node with an asterisk (\*) representing a value of 100. The first vertical bar indicates the results of the species delimitation analysis. The states of selected morphological characters are colour-coded with vertical bars on the right.

## Phylogenetic analysis and species delimitation

The maximum likelihood tree (Fig. 10; data available from FigShare) recovered Proneomeniidae as non-monophyletic, with *Dorymenia* and *Proneomenia* in two separate clades. *Dorymenia* was recovered as the sister taxon to a clade composed of Strophomeniidae Salvini-Plawen, 1978 (represented by *Anamenia gorgonophila* (Kowalevsky, 1880) in the tree)

and Epimeniidae Salvini-Plawen, 1978 (represented by *Epimenia australis* (Thiele, 1897) and *E. babai* Salvini-Plawen, 1978). This combined clade, including *Dorymenia*, Strophomeniidae and Epimeniidae but excluding *Proneomenia*, was well supported (bootstrap support, bs = 99%). *Proneomenia* was recovered as sister to the clade composed of *Dorymenia*, Strophomeniidae and Epimeniidae, albeit with weak support (bs = 67%). *Dorymenia, Proneomenia* 

and *Epimenia* Nierstrasz, 1908 each had full support for monophyly. Two representatives of Pruvotinidae Heath, 1911 and two representatives of Simrothiellidae Salvini-Plawen, 1978 that belong to the traditionally recognised order 'Cavibelonia', currently viewed as polyphyletic (Kocot *et al.* 2019), were also sampled. Both families were recovered as monophyletic with moderate to strong support. Pruvotinidae was recovered as the sister clade to the clade consisting of *Proneomenia*, Strophomeniidae, Epimeniidae and *Dorymenia*, although the bootstrap support for this grouping was only 77% (Fig. 10).

Species delimitation with ASAP recovered a best partitioning scheme (according to ASAP score that ranged from 2 to 12) that grouped the sampled taxa into 22 species (data available from FigShare) (Fig. 10). Each of the new species described here were recovered in a separate partition (species concept) with all three individuals of *Proneomenia franziae* sp. nov. recovered in the same partition, as predicted based on morphology. Most sampled taxa were the sole representative of the partition, consistent with our expectations based on morphology. Aside from *Proneomenia franziae* sp. nov., two other partitions included multiple individuals: (1) a partition including *Proneomenia* sp. indet. (ALMNH: Inv:24165) and *Proneomenia* sp. indet. (ALMNH: Inv:24163) to the exclusion of *Proneomenia gerlachei* (ALMNH:Inv:24161/Ap205.2E) and (2) a partition including *Epimenia australis* and *E. babai*.

#### Ancestral character state reconstruction

Using the reconstructed phylogeny, we performed ancestral character state reconstruction (Supplementary Fig. S1–S11) to make inferences about the evolution of characters commonly used in solenogaster taxonomy. Specifically, we sought to assess the taxonomic value of these characters and identify morphological support for what we refer to as the 'Proneomeniidae clade' (clade that includes *Proneomenia*, Strophomeniidae, Epimeniidae and *Dorymenia*) and the subclade including *Dorymenia*, Strophomeniidae and Epimeniidae but excluding *Proneomenia*.

Based on ancestral character state reconstruction, the 'Proneomeniidae clade' had an ancestor with a large body size (2-10 cm) and a rough habitus. The most recent common ancestor of the 'Proneomeniidae clade' most likely had type-C-Epimenia-type ventrolateral foregut glands, suggesting that the type-B-Imeroherpia-type of Strophomeniidae (represented here by *Anamenia gorgonophila*) is apomorphic. The radula of the ancestor of the 'Proneomeniidae clade' clade was most likely a polystichous radula, that was retained in Proneomenia and Dorymenia but underwent independent state changes to a pectinate or distichous radula in Epimeniidae and Strophomeniidae (according to the classification of radula types in García-Álvarez and Salvini-Plawen 2007). Additionally, if the radula of Anamenia is reinterpreted as distichous (see Discussion below), the presence of a distichous radula in the last common ancestor of Epimeniidae and Strophomeniidae with a secondary loss of the radula in *Strophomenia* is most parsimonious, although our likelihood-based ancestral character state reconstruction analysis favours a polystichous radula in the last common ancestor of the Epimeniidae-Strophomeniidae clade.

Copulatory stylets are an important character as the presence or absence is the main difference between Proneomenia and Dorymenia. Ancestral state reconstruction suggests that the most recent ancestor to the 'Proneomeniidae clade' lacked this structure, and therefore the most recent common ancestor of Dorymenia likely evolved copulatory stylets independently from other solenogaster taxa in the clade that bears these reproductive structures. Therefore this main difference between the two genera of interest does not, however, provide morphological synapomorphies for a clade of Dorymenia, Epimeniidae and Strophomeniidae. Most if not all species in the 'Proneomeniidae clade' lack respiratory folds (with at least *Proneomenia satiata* sp. nov. and *P*. franziae sp. nov. as possible exceptions), a character that is shared with the most recent common ancestor. All Proneomenia and Dorymenia species included in the analysis (except for D. boucheti sp. nov.) have between one and four seminal receptacles that coincide with the inferred state for the ancestor of the 'Proneomeniidae clade'. Our analysis indicates that Epimeniidae and Strophomeniidae evolved independently to have more than four seminal receptacles with the most recent common ancestor of Epimeniidae and Strophomeniidae likely having between one and four seminal receptacles. The ancestor of the 'Proneomeniidae clade' mostly likely had one or more dorsoterminal sensory organs. Notably, the apparent absence of these organs in some of the species included in the analysis could be attributed to the lack of quality of the histological sections (broken cuticle or overstained in the region of interest). According to the ancestral state reconstruction, whether the ancestor to the 'Proneomeniidae clade' had abdominal spicules or not is ambiguous. These structures are present in all the considered groups, although the lack of this structure in many of the Proneomenia species included in the analysis is noteworthy.

# **Discussion**

# Species identification and solenogaster diversity in the South China Sea

Given the currently accepted taxonomy of Solenogastres and based on the established diagnostic characters (García-Álvarez and Salvini-Plawen 2007), specimen identification was straightforward and classification within Proneomeniidae was clear based on the thick cuticle (>50 µm), layered organisation of hollow acicular sclerites, polystichous radula and type-C–Epimenia-type foregut glands. The presence or absence of copulatory stylets is the only character distinguishing the two genera of the family (García-Álvarez and Salvini-Plawen

2007; García-Álvarez *et al.* 2009). A comparison of the most relevant anatomical characters between the specimens from the South China Sea and the known species in the family was conducted. This confirmed that these all belong to four new species. As the material available for the present work consisted of only eight specimens and considering that proneomeniids are some of the largest solenogasters and therefore more likely to be noticed in trawled material than the small-bodied relatives, the real diversity in this region is likely higher. The only previously published record of Solenogastres from the South China Sea was an unidentified *Proneomenia* by the Marine Biological Museum of Chinese Academy of Sciences (Ocean Biodiversity Information System 2022).

Analyses of our DNA barcoding data proved useful to evaluate our morphospecies groupings, and family and genus-level identifications before histology was performed. In particular, Proneomenia occulta sp. nov. was initially thought to be another specimen of Dorymenia boucheti sp. nov. based on the external aspect and initial examination of sclerites. The external aspect of this specimen differed only slightly from the holotype of Dorymenia boucheti sp. nov. as this had no marked digitiform projections on the posterior end. We speculated that this smaller specimen represented a juvenile where this digitiform projection was not as well developed, as this has been pointed out as a possibility for other species (Scheltema et al. 2012). Phylogenetic analysis of the DNA barcodes obtained helped us to identify this as a Proneomenia instead, as supported by histology (lack of copulatory stylets). In addition, all the sectioned Antarctic specimens with copulatory stylets were recovered in the Dorymenia clade of the reconstructed phylogenetic tree, providing support for this character as diagnostic between the genera Dorymenia and Proneomenia. Furthermore, our species delimitation analysis recovered each of the new species described here in separate partitions, consistent with our inference based on morphology. Therefore our results demonstrate the utility of DNA barcoding of Solenogastres as a taxonomic tool to avoid underestimating biodiversity due to subtle external differences, for evaluating the utility of morphological characters for taxonomy and for evaluating species concept hypotheses.

# Evidence for paraphyly of Proneomeniidae

In addition to the utility as a taxonomic tool, DNA barcodes were useful to assess whether the accepted systematics of the taxa under consideration reflect the group's evolutionary history. Our analysis revealed the paraphyly of Proneomeniidae with respect to Epimeniidae and Strophomeniidae (Fig. 10). This separation of the two genera of the family is contradictory to the currently accepted family 'Proneomeniidae', that was proposed based on morphological characters (thick cuticle with epidermal papillae and hollow acicular sclerites inserted in several layers, a polystichous radula, foregut glands of type-C-Epimenia-type and at least one pair of

seminal receptacles). However, evidence for non-monophyly of Proneomeniidae has been published previously. Kocot *et al.* (2022) recently reported that, in Kocot *et al.* (2019), the specimen identified as *Entonomenia tricarinata* (Salvini-Plawen, 1978), which belongs to Rhopalomeniidae Salvini-Plawen, 1978, was actually *Dorymenia tricarinata* Heath, 1999, which belongs to Proneomeniidae, but has a similar habitus and an overlapping distribution. Interestingly, Kocot *et al.* (2019) recovered *Dorymenia tricarinata* Heath, 1911 as sister to *Epimenia* and that clade was recovered as sister to a clade composed of two *Proneomenia* spp. Given that *Anamenia* was not sampled by Kocot *et al.* (2019), these results are consistent with our results.

Admittedly, our study presents a phylogenetic analysis based on only two mitochondrial genes. Therefore revisiting this question in more detail in the future with expanded gene and taxon sampling to confirm this result would be interesting. The 'Proneomeniidae clade' (*Proneomenia + Dorymenia +* Strophomeniidae + Epimeniidae) contains 64 species (including the ones described here), only 11 of which (belonging to four of the six genera) were sampled in this work. Although this can be considered a reasonable number of taxa, increasing the number of taxa sampled for Strophomeniidae, Epimeniidae and other potentially related groups would be desirable

## Remarks on the 'Proneomeniidae clade'

Ancestral character state reconstruction analyses are useful to understand the evolution of characters traditionally used in solenogaster taxonomy and therefore to evaluate the taxonomic value and utility to explain the recovered groups in our phylogenetic analysis (with special focus on what we will refer to as the 'Proneomeniidae clade' that includes Proneomenia, Strophomeniidae, Epimeniidae and Dorymenia). Traditionally, ventrolateral foregut glands and the radula are the most important taxonomic characters at the family level, and the combination of these two characters with the presence or absence of other internal anatomical characters (e.g. seminal receptacles, respiratory folds, copulatory stylets or dorsoterminal sensory organs) are useful to define genera (García-Álvarez and Salvini-Plawen 2007). Following this, the groupings we recovered at what is traditionally considered 'genus-level' are quite clear and correlate with the established morphological diagnoses of these genera (Fig. Supplementary Fig. S1-S11). However, although our phylogenetic analysis strongly indicates that Proneomenia and Dorymenia do not constitute a monophyletic group, our scrutiny of morphological characters failed to reveal clear synapomorphies for a clade of Dorymenia, Strophomeniidae and Epimeniidae to the exclusion of Proneomenia, despite strong support for this grouping in our analyses. On the other hand, although our phylogenetic analysis resulted in weak support for the node defining the 'Proneomeniidae clade', ancestral character state reconstruction indicates that the

following shared characters are considered diagnostic for this group: (a) body size and general habitus; (b) ventrolateral foregut glands; (c) radula; (d) seminal receptacles; (e) respiratory folds; (f) dorsoterminal sensory organs; (g) copulatory stylets; and (h) abdominal spicules.

Traditionally, the diagnosis of families and genera does not include details on the habitus. However, in our opinion this should be included because, as shown in this study, these may be relevant to diagnosing the clades. The 'Proneomeniidae clade' includes the largest known species of Solenogastres (*Epimenia babai*, that can reach 300 mm long and 10 mm in diameter; Salvini-Plawen 1997). Although there are some smaller-bodied exceptions (e.g. *Dorymenia boucheti* sp. nov. that is only 12.5 mm and *Proneomenia custodiens* that is 10 mm), in general, members of this clade are large-bodied animals between 30 and 150 mm long. The 'Proneomeniidae clade' is represented by stout animals in which the sclerites form a thick covering and do not protrude or protrude only slightly from the thick cuticle, giving these a rough aspect.

Ventrolateral foregut glands are complicated structures, the function of which is related to digestion. Therefore, the variability may be related to trophic niche specialisation (Bergmeier et al. 2021). The traditional classification of these organs, first proposed by Salvini-Plawen (1978), uses single letters to name the different types. This classification was refined by Handl and Todt (2005) by naming each type after the genus in which this was first described. In addition, Handl and Todt (2005) stated that 'gross morphology and anatomy of the ventrolateral foregut glands constitute useful taxonomic characters in determining higher taxa (family level), and finer details of the anatomy and cytology are useful in determining lower levels (genus and species)'. In the 'Proneomeniidae clade' there are two types of ventrolateral foregut glands and, according to our results, the most recent common ancestor had type-C-Epimenia-type ventrolateral foregut glands that were secondarily modified to type-B-Imeroherpia-type glands in Strophomeniidae. Ventrolateral foregut glands, particularly the Epimenia-type, are usually long organs that are not always completely reconstructed, as only a portion of the anterior part of the animal is usually sectioned. This is especially important if we consider the so-called type-B, characteristic of Strophomeniidae (along with Imeroherpia, Heteroherpia and Syngenoherpia; Salvini-Plawen, 1978). Handl and Todt (2005) analysed this type in the species Imeroherpia laubieri Handl, 2002 and described these as 'ventrolateral foregut glands with extraepithelial glandular cells and inner and outer musculature'. The special case of Syngenoherpia in which intraepithelial glandular cells (as in the type-C-Epimenia-type) occur in the anterior parts of the glands, whereas the extraepithelial glandular cells and inner and outer musculature occur in the posterior region (Salvini-Plawen 1978; Syngenoherpia-type Handl and Todt 2005) was also pointed out. This is particularly relevant since Salvini-Plawen (1997) described the ventrolateral organs of one specimen of Epimenia australis (as E. verrucosa; see

fig. 58 in Salvini-Plawen 1997) as type-C but with 'distal portions of gland cells interspersed with muscle fibres (simulating glandular organs of type-B) and terminal portion without gland cells and those interspersed fibres unite with surrounding musculature'. The importance of avoiding overgeneralisation and including detailed descriptions of ventro-lateral foregut glands, as advocated by Handl and Todt (2005) is emphasised here as available information is limited for this clade. More detailed studies would be desirable to obtain a deeper insight into the evolution and diversity of the ventro-lateral foregut glands in the 'Proneomeniidae clade', especially to confirm whether more species of this group have modified organs such as those of *Epimenia australis*, that would mean there is a single type of these organs for the 'Proneomeniidae clade' but with specific modifications in some genera.

The conventionally used classification system of the radula in solenogasters consists of five types (reviewed by García-Álvarez and Salvini-Plawen 2007) based on the assumption of a lack of a 'true' radular membrane (Wolter 1992) and therefore the classification of radula types was built on the number and shape of the teeth (Salvini-Plawen 1978; Handl 2002). On the contrary, other authors endorse the existence of a radular membrane, with the lack of rhachidian tooth and a subradular membrane as the difference between aplacophorans and the other molluscan classes (Scheltema 1988; Scheltema et al. 2003). These authors suggest three radula types built on the concepts of a 'unipartite radula' (single structure applied to either or both the teeth and the membrane) and a 'bipartite radula' (paired, mirror-image structure applied both to teeth and the membrane that can be partially or completely divided). Therefore the biserial and distichous types of the García-Álvarez and Salvini-Plawen (2007) classification system are viewed here as special cases of the distichous type of Scheltema (1988). According to García-Álvarez and Salvini-Plawen (2007) there are three different radula types in the 'Proneomeniidae clade'. These include the polystichous radula in Dorymenia and Proneomenia (many-toothed radula with a membrane that can either be unipartite or bipartite; Scheltema et al. 2003), the distichous radula in Epimeniidae (distichous with a unipartite membrane; Scheltema et al. 2003) and a biserial pectinate radula in Anamenia (exclusive to this genus). García-Álvarez and Salvini-Plawen (2007) included the pectinated type of Anamenia in the biserial type, thereby implying a distichous type according to Scheltema's (1988) classification system and therefore of the same type as in Epimenia. The radula in Anamenia has not been studied a great deal (Scheltema et al. 2003) and the existing descriptions raise doubts about the unipartite or bipartite nature of the radular membrane (if the existence is assumed) and whether there is a junction (symphysis) between the teeth (compiled in Saito and Salvini-Plawen 2010, table 1). Most commonly in solenogasters the information we have about the radula is derived from histological sections, that makes the analysis of this structure complicated as teeth often break during histological

studies. Therefore, interpretations of the shape, number of denticles, size, etc., can be ambiguous. Examining radulae that have been extracted and whole-mounted is a valuable alternative to histology but this is challenging due to the fragility and small size. In the description of Anamenia amabilis Saito & Salvini-Plawen, 2010, the authors obtained an entire radula (Saito and Salvini-Plawen 2010, fig. A) and interpret this as a biserial radula with two separate teeth. Nevertheless, in view of the sections, drawings and photographs of extracted radulae in the literature, the differences between the 'pectinate' radula of Anamenia and the radula of Epimenia (e.g. figures in Salvini-Plawen 1997) are not clearly distinct. Our observations of the radula of Anamenia gorgonophila (histological sections) also suggest the existence of a junction (symphysis) between the teeth. Therefore Anamenia and Epimenia can be interpreted to have the same radula type with hypertrophied denticles in Anamenia. The absence of a radula in Strophomenia Pruvot, 1899 (the other genera within Strophomeniidae and traditionally differentiated from Anamenia by the lack of radula) must be pointed out but, assuming placement as the sister taxon to Anamenia, this absence is most parsimoniously interpreted as a secondary loss.

Although ventrolateral foregut glands and the radula tend to be consistent within solenogaster families (García-Álvarez and Salvini-Plawen 2007), there are exceptions. For example, in Pruvotinidae there is variation in the type of foregut glands and radula among the genera with the ventrolateral foregut glands being determinant between subfamilies and with some genera lacking a radula (García-Álvarez and Salvini-Plawen 2007; Pedrouzo et al. 2022). In Simrothiellidae, the type of foregut glands varies among genera (García-Álvarez and Salvini-Plawen 2007) and although these share the same general type of radula, there is notable variation in arrangement and shape. Taken together, the variability in the ventrolateral foregut glands and radula in the 'Proneomeniidae clade' and in these two families indicates that these characters are more evolutionarily labile than previously known.

Respiratory folds are variably present in Solenogastres and do not appear to be correlated with body size as at least most members of the generally large-bodied 'Proneomeniidae clade' lack these structures. However, our examination of Proneomenia satiata sp. nov. and P. franziae sp. nov. reveals these as a possible exception, the pallial cavity epithelium of which contains folds that, although differing in appearance from the respiratory folds and papillae known in other solenogasters, may serve a function in gas exchange. Knowing more about the putative respiratory folds of these species from the study of more material and further learning about the ecology would be of interest. The diagnosis of Proneomenia in the literature states that respiratory folds are lacking and we have not amended this here given our uncertainty about the function of these folds, but we wish to emphasise this observation to raise awareness of the issue.

The dorsoterminal sensory organ(s) are located in the posterior region of the body, opening to the exterior through the cuticle. Given the presumed chemosensory function and proximity to the reproductive organs, a role during copulation has been hypothesised for these organs (Haszprunar 1987) and these may not be fully developed in juvenile specimens (Bergmeier et al. 2016). Even when fully developed, locating these structures in histological sections (e.g. if the cuticle is damaged or if the organ is small relative to the thickness of the sections) may be difficult. Therefore, the presence or absence of this organ should be interpreted with caution, especially when limited histological data are available as is often the case. The ancestor of the 'Proneomeniidae clade' most likely had dorsoterminal sensory organ(s) and the apparent absence in some species examined here may be due to the issues mentioned, providing another argument for the importance of studying multiple specimens when possible. Given the information available, the presence or absence of dorsoterminal sensory organs and the number may be valuable characters at the species level but this does not appear to be reliable for higher-level taxonomy.

Due to the role in reproduction, the size, shape and appearance of the seminal receptacles in histological sections can be considered dependent on the state of maturity of the individuals. Additionally, the quality of the sections may prevent characterisation. Therefore, the absence of these structures and the taxonomic significance should be interpreted with caution. All the species of the 'Proneomeniidae clade' included in the analysis (except for one) have at least one pair of seminal receptacles, that coincides with the inferred state for the ancestor of the 'Proneomeniidae clade' and with other species in this group not included in the analysis. Epimeniidae and Strophomeniidae seem to have evolved bundles of more than four seminal receptacles attached to each pericardioduct; these are estimated to be two separate changes.

Copulatory stylets occur in several distantly related clades of solenogasters (García-Álvarez and Salvini-Plawen 2007). Owing to the role during copulation, great taxonomic value has been attributed to these, particularly at the genus level. The presence of copulatory stylets in *Dorymenia* is the only diagnostic difference from *Proneomenia*. In the 'Proneomeniidae clade', copulatory stylets are exclusively found in *Dorymenia*, meaning this character was lost in in *Proneomenia*, Epimeniidae and Strophomeniidae or, more parsimoniously, secondarily gained in *Dorymenia*.

Abdominal spicules are elongated sclerites arranged in bundles at both sides of the opening of the pallial cavity. These are assumed to be involved in reproduction but the function has not been addressed well. This character is not included in diagnoses at the family or genus levels. However, we included this here as Salvini-Plawen (1997) pointed out the similarities in these structures in Epimeniidae, Strophomeniidae and Proneomeniidae. Owing to the size of the animals in these

groups, these structures have been studied in detail for several species by researchers who extracted the animals intact rather than inferring the structure and organisational histology (Scheltema *et al.* 2012; Todt and Kocot 2014; Pedrouzo *et al.* 2019). However, abdominal spicules have been found in many solenogaster taxa and described based only on serial sections. Therefore, more studies are needed to be able to compare the spicules of the 'Proneomeniidae clade' with those found in other groups. Although abdominal spicule presence seems to be a character diagnostic of the 'Proneomeniidae clade', as for the dorsoterminal sensory organ, presence or absence can be diagnostic at genus level and particularities (e.g. number, position or shape of the spicules), characteristic of each species.

In addition to these characters, sclerites are also relevant. Mantle characteristics were central to the classification system of Salvini-Plawen (1978) and these were even considered important in earlier solenogaster studies (Nierstrasz 1902). The importance of sclerites for taxonomy has been echoed by several authors (e.g. Scheltema et al. 2012; Kocot and Todt 2014; Cobo and Kocot 2021), especially for the identification of higher taxa (Scheltema et al. 2012) and molecular phylogenetic analyses conducted to date are consistent with this view (e.g. Kocot et al. 2019; Bergmeier et al. 2021). In the 'Proneomeniidae clade', dominant mantle spicules are thick, hollow acicular sclerites, some of which have a slightly S-shaped curvature. Among these sclerites may be other elements such as solid paddle-shaped or hatched-shaped sclerites, such as those present in both Proneomenia or Dorymenia species or small lanceolate scales, such as those around the dorsoterminal sense organ in Epimenia (e.g. Epimenia babai Salvini-Plawen, 1997).

#### **Conclusions**

Here, we expand knowledge on the diversity of the solenogaster family Proneomeniidae and diversity of Solenogastres in the South China Sea including the description of four new species. Phylogenetic analysis of molecular data obtained from these specimens, and other members of Proneomeniidae and relevant outgroups recovered representatives of two other families (Epimeniidae and Strophomeniidae) nested within Proneomeniidae with strong support. In view of this, we conducted ancestral character state reconstruction and considered morphological characters potentially diagnostic for this clade that we refer to as the 'Proneomeniidae clade' and subclades.

Taken together, the 'Proneomeniidae clade' can be diagnosed by large body size, habitus, main sclerite type, ventrolateral foregut glands and radula (albeit with some variability and exceptions in these two characters) and the states of the other characters discussed here (seminal receptacles, respiratory folds, dorsoterminal sensory organs, copulatory stylets and abdominal spicules) as diagnostic of the

genera. Nevertheless, a deeper investigation of the phylogeny is needed to confirm our inferred phylogenetic relationships and determine the validity of the diagnostic characters proposed here, thereby providing guidance for revisionary systematics of this clade.

Particularly relevant for proposing a new classification would be to improve, besides gene sampling, the sampling of species within the 'Proneomeniidae clade' and putative relatives. In addition to more Anamenia species, representatives of Strophomenia (without radula) should be studied. In addition to more Epimenia species, adding and studying Epiherpia vixignis (Salvini-Plawen, 1978), the only species of the other genus of Epimeniidae for which important characters such as copulatory stylets are unknown, would be ideal. Two families can be considered putative relatives of the 'Proneomeniidae clade': Syngenoherpiidae Salvini-Plawen, 1978 and Rhipidoherpiidae Salvini-Plawen, 1978. Both have an external appearance and sclerites that are similar to those of the 'Proneomeniidae clade'. The former is monogeneric (Syngenoherpia Salvini-Plawen, 1978) with ventrolateral foregut glands of type-B, seminal receptacles in bundles, copulatory stylets, dorsoterminal sensory organs and respiratory folds. In addition, the radula of the species of this family has been described as 'distichous to biserial' (García-Álvarez and Salvini-Plawen 2007). Rhipidoherpiidae is characterised by a polystichous radula, ventrolateral foregut glands of type-A and seminal receptacles in bundles. This family includes two genera: Rhipidoherpia Salvini-Plawen, 1978 (with copulatory stylets, dorsoterminal sensory organ and without respiratory folds) and Thieleherpia Salvini-Plawen, 2004 (without copulatory stylets or respiratory folds and with a dorsoterminal sensory organ). Moreover, Thieleherpia thulensis (Thiele, 1900), that was originally included in Proneomeniidae, has many similarities with Proneomenia custodiens (K. M. Kocot, pers. obs.), with the ventrolateral foregut glands being the main difference between the species. More comprehensive sampling would be valuable with respect to gaining a better understanding of the phylogenetic relationships of these taxa, inferring ancestral character states and identifying characters that are or are not diagnostic of monophyletic groups in this part of the solenogaster tree.

# **Supplementary material**

Supplementary material is available online.

## References

Bergmeier FS, Haszprunar G, Tod C, Jörger KM (2016) Lost in a taxonomic Bermuda Triangle: comparative 3D-microanatomy of cryptic mesopsammic Solenogastres (Mollusca). *Organisms, Diversity & Evolution* **16**(3), 613–639. doi:10.1007/s13127-016-0266-6

Bergmeier FS, Brandt A, Schwabe E, Jörger KM (2017) Abyssal Solenogastres (Mollusca, Aplacophora) from the Northwest Pacific: scratching the surface of deep-sea diversity using integrative

taxonomy. Frontiers in Marine Science 4, 410. doi:10.3389/fmars. 2017.00410

- Bergmeier FS, Haszprunar G, Brandt A, Saito H, Kano Y, Jörger KM (2019) Of basins, plains, and trenches: systematics and distribution of Solenogastres (Mollusca, Aplacophora) in the Northwest Pacific. *Progress in Oceanography* **178**, 102187. doi:10.1016/j.pocean.2019. 102187
- Bergmeier FS, Ostermair L, Jörger KM (2021) Specialized predation by deep-sea Solenogastres revealed by sequencing of gut contents. *Current Biology* **31**(13), R836–R837. doi:10.1016/j.cub.2021. 05.031
- Cobo MC, Kocot KM (2020) Micromenia amphiatlantica sp. nov.: first solenogaster (Mollusca, Aplacophora) with an amphi-Atlantic distribution and insight into abyssal solenogaster diversity. Deep-Sea Research I. Oceanographic Research Papers 157, 103189. doi:10.1016/j.dsr.2019.103189
- Cobo MC, Kocot KM (2021) On the diversity of abyssal Dondersiidae (Mollusca: Aplacophora) with the description of a new genus, six new species, and a review of the family. *Zootaxa* **4933**(1), 63–97. doi:10.11646/zootaxa.4933.1.3
- De Oliveira AL, Wollesen T, Kristof A, Scherholz M, Redl E, Todt C, Bleidorn C, Wanninger A (2016) Comparative transcriptomics enlarges the toolkit of known developmental genes in mollusks. *BMC Genomics* **17**, 905. doi:10.1186/s12864-016-3080-9
- Folmer O, Black M, Hoeh W, Lutz R, Vrijenhoek R (1994) DNA primers for amplification of mitochondrial cytochrome *c* oxidase subunit I from diverse metazoan invertebrates. *Molecular Marine Biology and Biotechnology* **3**, 294–299.
- García-Álvarez O, Salvini-Plawen L (2007) Species and diagnosis of the families and genera of Solenogastres (Mollusca). *Iberus* **25**(2), 73–143.
- García-Álvarez O, Urgorri V (2003) Solenogastres molluscs from the BENTART Collection (South Shetland Islands, Antarctica), with a description of a new species. *Iberus* **21**(1), 43–56.
- García-Álvarez O, Urgorri V, von Salvini-Plawen L (2000) Two new species of *Dorymenia* (Mollusca: Solenogastres: Proneomeniidae) from the South Shetland Islands (Antarctica). *Journal of the Marine Biological Association of the United Kingdom* **80**(5), 835–842. doi:10.1017/S0025315400002812
- García-Álvarez O, Zamarro M, Urgorri V (2009) Proneomeniidae (Solenogastres, Cavibelonia) from the Bentart-2006 Expedition, with description of a new species. *Iberus* **27**(1), 67–78.
- García-Álvarez O, Salvini -Plawen L, Urgorri V (2014) Solenogastres. In 'Fauna Iberica. Vol. 38. Mollusca Solenogastres, Caudofoveata, Monoplacophora'. (Eds García-Álvarez O, Salvini-Plawen L, Urgorri, V, Souza Troncoso J) pp. 11–26 (Museo Nacional de Ciencias Naturales. CSIC: Madrid, Spain) [In Spanish]
- Gil-Mansilla E, García-Álvarez O, Urgorri V (2008a) New Acanthomeniidae (Solenogastres, Cavibelonia) from the abyssal Angola Basin. *Zootaxa* **1866**, 175–186.
- Gil-Mansilla E, García-Álvarez O, Urgorri V (2008b) Metodología para la recolección, conservación y estudio de los moluscos Solenogastros. [Methodology for the collection, conservation and study of Solenogastres molluscs.] *Reseñas Malacológicas XIII*, 1–31. [In Spanish]
- Gil-Mansilla E, García-Álvarez O, Urgorri V (2009) A new genus and two new species of Simrothiellidae (Solenogastres: Cavibelonia) from the Abyssal Angola Basin. *Journal of the Marine Biological Association of the United Kingdom* **89**(7), 1507–1515. doi:10.1017/S0025315409000666
- Handl CH (2002) Imeroherpia laubieri, a new solenogaster from the Bay of Biscay. Journal of Molluscan Studies 68, 329–335. doi:10.1093/ mollus/68.4.329
- Handl CH, Todt C (2005) Foregut glands of Solenogastres (mollusca): anatomy and revised terminology. *Journal of Morphology* **265**(1), 28–42. doi:10.1002/jmor.10336
- Haszprunar G (1987) The fine morphology of the osphradial sense organs of the Mollusca. IV. Caudofoveata and Solenogastres. *Philosophical Transactions of the Royal Society of London B. Biological Sciences* **315**(1169), 63–73. doi:10.1098/rstb.1987.0003
- Heath H (1905) The morphology of a solenogastre. Zoologische Jahrbücher. Abteilung für Anatomie und Ontogenie der Tiere Abteilung für Anatomie und Ontogenie der Tiere 21(4), 701–734.

- Heath H (1911) Reports on the scientific results of the expedition to the Tropical Pacific, in charge of Alexander Agassiz, by the US Fish Commission Steamer Albatross, from August 1899 to June 1900, Commander Jefferson F. Moser. XVI. 'The Solenogastres.'. Memoirs of the Museum of Comparative Zoology at Harvard College, 45, 1–182.
- Heath H (1918) Solenogastres from the eastern coast of North America.

  Memoirs of the Museum of Comparative Zoology at Harvard College 45(2), 187–360.
- Hubrecht A (1880) Proneomenia sluiteri g. et sp. n. g. & sp. nn. Zoologischer Anzeiger 3, 589–590.
- Katoh K, Standley DM (2013) MAFFT multiple sequence alignment software version 7: improvements in performance and usability. *Molecular Biology and Evolution* **30**(4), 772–780. doi:10.1093/molbev/mst010
- Kocot KM, Todt C (2014) Three new meiofaunal solenogaster species (Mollusca: Aplacophora) from the north-east Pacific. *Journal of Natural History* **48**(45–48), 3007–3031. doi:10.1080/00222933. 2014.961987
- Kocot KM, Cannon JT, Todt C, Citarella MR, Kohn AB, Meyer A, Santos SR, Schander C, Moroz LL, Lieb B, Halanych KM (2011) Phylogenomics reveals deep molluscan relationships. *Nature* **477** (7365), 452–456. doi:10.1038/nature10382
- Kocot KM, Todt C, Mikkelsen NT, Halanych KM (2019) Phylogenomics of Aplacophora (Mollusca, Aculifera) and a solenogaster without a foot. *Proceedings of the Royal Society of London B. Biological Sciences* **286**(1902), 20190115. doi:10.1098/rspb.2019.0115
- Kocot KM, Todt C, Mikkelsen NT, Halanych KM (2022) Correction to: 'Phylogenomics of Aplacophora (Mollusca, Aculifera) and a solenogaster without a foot' (2019) by Kocot et al. Proceedings of the Royal Society of London B. Biological Sciences 289(1986), 20190115. doi:10.1098/rspb.2022.2057
- Koren J, Danielssen DC (1877) Beskrivelse over nye arter, henhørende til slaegten *Solenopus*, samt nogle oplysninger om dens organisation. [Description of new species, belonging to the genus *Solenopus*, as well as some information on its organisation.] *Journal of Natural History* **3**(17), 321–328. [In Danish]
- Kowalevsky A, Marion A (1887) Contributions à l'histoire des Solénogastres ou Aplacophores. [Contributions to the history of the Solenogastres or Aplacophores.] *Annales du Musée d'Histoire Naturelle de Marseille, Zoologie* **3**(1), 1–77. [In French]
- Lewis PO (2001) A likelihood approach to estimating phylogeny from discrete morphological character data. *Systematic Biology* **50**, 913–925. doi:10.1080/106351501753462876
- McCutcheon MG, Kocot KM, Cobo MC (2022) Uncovering the biodiversity of Solenogastres (Mollusca, Aplacophora) with three new species of Proneomeniidae Simroth, 1893 and new data for *Dorymenia quincarinata* (Ponder, 1970). *Molluscan Research* 42(4), 271–286. doi:10.1080/13235818.2022.2143069
- Martínez-Sanjuán J, Kocot K, García-Álvarez Ó, Candás M, Díaz-Agras G (2022) Computed microtomography (Micro-CT) in the anatomical study and identification of Solenogastres (Mollusca). *Frontiers in Marine Science* **8**, 760194. doi:10.3389/fmars.2021.760194
- Mikkelsen NT, Kocot KM, Halanych KM (2018) Mitogenomics reveals phylogenetic relationships of caudofoveate aplacophoran molluscs. *Molecular Phylogenetics and Evolution* **127**, 429–436. doi:10.1016/j. ympev.2018.04.031
- Mikkelsen NT, Todt C, Kocot KM, Halanych KM, Willassen E (2019) Molecular phylogeny of Caudofoveata (Mollusca) challenges traditional views. *Molecular Phylogenetics and Evolution* **132**, 138–150. doi:10.1016/j.ympev.2018.10.037
- Minh BQ, Schmidt HA, Chernomor O, Schrempf D, Woodhams MD, von Haeseler A, Lanfear R (2020) IQ-TREE 2: new models and efficient methods for phylogenetic inference in the genomic era. *Molecular Biology and Evolution* 37(5), 1530–1534. doi:10.1093/molbev/msaa015
- Mora C, Tittensor DP, Adl S, Simpson AGB, Worm B (2011) How many species are there on Earth and in the ocean? *PLoS Biology* **9**(8), e1001127. doi:10.1371/journal.pbio.1001127
- Nierstrasz H (1902) The Solenogastres of the Siboga-Expedition. Siboga-Expeditie 47, 1–46.
- Ocean Biodiversity Information System (2022) Observation data collected by Marine Biological Museum, Chinese Academy of Sciences (SCS-Part II). (OBIS, Intergovernmental Oceanographic Commission of UNESCO) Available at <a href="https://www.obis.org/dataset/e68c1476-8ef3-4836-9306-c929e05a58f2">www.obis.org/dataset/e68c1476-8ef3-4836-9306-c929e05a58f2</a>

Okusu A, Schwabe E, Eernisse DJ, Giribet G (2003) Towards a phylogeny of chitons (Mollusca, Polyplacophora) based on combined analysis of five molecular loci. *Organisms Diversity & Evolution* **3**(4), 281–302. doi:10.1078/1439-6092-00085

- Ostermair L, Brandt A, Haszprunar G, Jörger KM, Bergmeier FS (2018) First insights into the solenogaster diversity of the Sea of Okhotsk with the description of a new species of *Kruppomenia* (Simrothiellidae, Cavibelonia). *Deep-Sea Research II. Topical Studies in Oceanography* **154**, 214–229. doi:10.1016/j.dsr2.2017.12.008
- Pedrouzo L, Cobo MC, García-Álvarez Ó, Rueda JL, Gofas S, Urgorri V (2014) Solenogastres (Mollusca) from expeditions off the South Iberian Peninsula, with the description of a new species. *Journal of Natural History* **48**, 2985–3006. doi:10.1080/00222933.2014.959576
- Pedrouzo L, García-Álvarez Ó, Urgorri V, Pérez-Señarís M (2019) New data and 3D reconstruction of four species of Pruvotinidae (Mollusca: Solenogastres) from the NW Iberian peninsula. *Marine Biodiversity* **49**(1), 277–287. doi:10.1007/s12526-017-0793-1
- Pedrouzo L, García-Álvarez Ó, Urgorri V (2022) New species of Pruvotininae (Solenogastres, Cavivelonia) from bathyal bottoms off the NW Iberian Peninsula, with a taxonomical discussion about the family Provotinidae. *Iberus* **40**(2), 317–354.
- Pelseneer P (1901) Les Néoméniens de l'Expédition Antarctique Belge et la distribution géographique des Aplacophora. [The Neomenians of the Belgian Antarctic Expedition and the geographical distribution of Aplacophora.] Bulletin de la Classe des sciences 9–10, 528–534. [In French]
- Ponder WF (1970) A new aplacophoran from New Zealand. *Journal of the Malacological Society of Australia* **2**(1), 47–54. doi:10.1080/00852988.1970.10673840
- Puillandre N, Brouillet S, Achaz G (2021) ASAP: assemble species by automatic partitioning. *Molecular Ecology Resources* **21**, 609–620. doi:10.1111/1755-0998.13281
- Revell LJ (2012) phytools: an R package for phylogenetic comparative biology (and other things). *Methods in Ecology and Evolution* **3**, 217–223. doi:10.1111/j.2041-210X.2011.00169.x
- Saito H, Salvini-Plawen L (2010) A new species of Anamenia (Mollusca: Solenogastres: Cavibelonia) from southern Japan. *Venus* **69**(1–2), 1–15.
- Salvini-Plawen L (1978) Antarktische und Subantarktische Solenogastres eine monographie: (1898–1974). [Antarctic and Subantarctic Solenogastres a monograph: (1898–1974).] *Zoologica* **128**, 1–315. [In German]
- Salvini-Plawen L (1985) Early evolution and the primitive groups. In 'The Mollusca. Vol. 10. Evolution'. (Eds ER Trueman, MR Clarke) pp. 59–150. (Academy Press: Orlando, FL, USA)
- Salvini-Plawen L (1997) Systematic revision of the Epimeniidae (Mollusca: Solenogastres). *Journal of Molluscan Studies* **63**(2), 131–155. doi:10.1093/mollus/63.2.131
- Salvini-Plawen L (2003) On the phylogenetic significance of the aplacophoran Mollusca. *Iberus* 21, 67–97.
- Salvini-Plawen L, Steiner G (2014) The Testaria concept (Polyplacophora + Conchifera) updated. *Journal of Natural History* **48**(45-48), 2751–2772. doi:10.1080/00222933.2014.964787
- Scheltema AH (1988) Ancestors and descendants relationships of the Aplacophora and Polyplacophora. *American Malacological Bulletin* **6**(1), 57–68.

- Scheltema AH (1992) The Aplacophora: history, taxonomy, phylogeny, biogeography, and ecology. PhD thesis, Woods Hole Oceanographic Institution, MA, USA.
- Scheltema AH, Ivanov DL (2000) Prochaetodermatidae of the eastern Atlantic Ocean and Mediterranean Sea (Mollusca: Aplacophora). *Journal of Molluscan Studies* **66**(3), 313–362. doi:10.1093/mollus/66.3.313
- Scheltema AH, Jebb M (1994) Natural history of a solenogaster mollusc from Papua New Guinea, *Epimenia australis* (Thiele) (Aplacophora: Neomeniomorpha). *Journal of Natural History* **28**(6), 1297–1318. doi:10.1080/00222939400770661
- Scheltema AH, Schander C (2000) Discrimination and phylogeny of solenogaster species through the morphology of hard parts (Mollusca, Aplacophora, Neomeniomorpha). *The Biological Bulletin* **198**(1), 121–151. doi:10.2307/1542810
- Scheltema AH, Kerth K, Kuzirian AM (2003) Original molluscan radula: comparisons among Aplacophora, Polyplacophora, Gastropoda, and the Cambrian fossil *Wiwaxia corrugata*. *Journal of Morphology* **257**(2), 219–245. doi:10.1002/jmor.10121
- Scheltema AH, Schander C, Kocot KM (2012) Hard and soft anatomy in two genera of Dondersiidae (Mollusca, Aplacophora, Solenogastres). *The Biological Bulletin* **222**(3), 233–269. doi:10.1086/BBLv222n3p233
- Smith SA, Wilson NG, Goetz FE, Feehery C, Andrade SCS, Rouse GW, Giribet G, Dunn CW (2011) Resolving the evolutionary relationships of molluscs with phylogenomic tools. *Nature* **480**(7377), 364–367. doi:10.1038/nature10526
- Thiele J (1903) Proneomenia valdiviae n. sp. Wissenschaftliche Ergebnisse der Deutschen Tiefsee-Expedition auf dem Dampfer "Valdivia" 1898–1899 3, 167–174. [In German] doi:10.5962/bhl. title.2171
- Todt C (2013) Aplacophoran mollusks—still obscure and difficult? American Malacological Bulletin 31(1), 181–187. doi:10.4003/006. 031.0110
- Todt C, Kocot KM (2014) New records for the solenogaster *Proneomenia sluiteri* (Mollusca) from Icelandic waters and description of *Proneomenia custodiens* sp. n. *Polish Polar Research* **35**(2), 291–310. doi:10.2478/popore-2014-0012
- Vinther J, Sperling EA, Briggs DEG, Peterson KJ (2012) A molecular palaeobiological hypothesis for the origin of aplacophoran molluscs and their derivation from chiton-like ancestors. *Proceedings of the Royal Society of London B. Biological Sciences* **279**(1732), 1259–1268. doi:10.1098/rspb.2011.1773
- Wirén A (1892) Studien über die Solenogastren. II. Chaetoderma productum, Neomenia, Proneomenia acuminata. [Studies on the Solenogastra. II. Chaetoderma productum, Neomenia, Proneomenia acuminata.] Kungliga Svenska Vetenskaps-Akademiens Handlingar 25(6), 1–99. [In German]
- Wolter K (1992) Ultrastructure of the radula apparatus in some species of aplacophoran molluscs. *Journal of Molluscan Studies* **58**(3), 245–256. doi:10.1093/mollus/58.3.245
- Zamarro M, García-Álvarez O, Urgorri V (2019) Biodiversity of the genus *Hemimenia* (Mollusca, Solenogastres, Neomeniamorpha) in Galician waters (NW Spain) with the description of three new species. *Iberus* **37**(2), 177–207.

Data availability. The data that support this study are available in the article and accompanying online supplementary material. Data related to the phylogenetic analysis, species delimitation analysis and ancestral character state reconstruction analysis have been uploaded to FigShare (https://doi.org/10.6084/m9.figshare.22216837.v1). The specimens studied are deposited in the Muséum National d'Histoire Naturelle (Paris, France) and the Alabama Museum of Natural History (Tuscaloosa, USA).

Conflicts of interest. The authors declare that they have no conflicts of interest.

Declaration of funding. This research was funded by the Fulbright Program (Ruth Lee Kennedy), the Malacological Society of London (Early Career Research Grant 2018), the Society of Systematic Biologists and the National Science Foundation (DEB-1846174). The French—Taiwanese deep-sea project TF-DeepEvo was funded by ANR and NSC (ANR 12-ISV7-0005-01). The Antarctic material was collected as part of the Icy Inverts cruises aboard the RV Lawrence M. Gould and RVIB Nathaniel B. Palmer funded by the National Science Foundation (ANT-1043745).

Acknowledgements. The South China Sea samples constitute a loan from the Muséum National d'Histoire Naturell. We thank Dr Philippe Bouchet and Dr Philippe Maestrati for their welcoming during Dr Cobo's stay in the Muséum National d'Histoire Naturell. The material from the South China Sea was collected as part of the French–Taiwanese deep-sea project TF-DeepEvo funded by ANR and NSC (ANR 12-ISV7-0005-01, Pls Sarah Samadi, Wei-Jen Chen). The Antarctic material was collected as part of the Icy Inverts cruises aboard the R/V Lawrence M. Gould and R/VIB Nathaniel B. Palmer (Dr Ken Halanych, chief scientist). The Icelandic material was collected as part of the IceAGE I cruise aboard the R/V Meteor (Dr Saskia Brix, chief scientist). We thank Christiane Todt for sharing specimens of Dorymenia sarsii. We also thank Will Farris for assistance in the lab and Dr Daryl Lam for assistance with ancestral character state reconstruction analyses. Finally, we thank Dr Franzi Bergmeier for helpful review and advice that greatly improved this manuscript.

#### **Author affiliations**

<sup>A</sup>Department of Biological Sciences, The University of Alabama, Tuscaloosa, AL, USA.

<sup>&</sup>lt;sup>B</sup>Alabama Museum of Natural History, The University of Alabama, Tuscaloosa, AL, USA.